Appendix A.

Two and Three Components Resonant Tanks

In this part, resonant tank with two and three resonant components will be listed and classified. Since this is a complex task, several boundaries were set to make it manageable.

First, assume variable frequency control is the control method going to be used for these tanks,

Second, for the resonant tank, input and output source type will be determined by tank configuration. For example, the output is must a current source for PRC since the primary side is capacitor, although PRC with voltage source could also work. This also means that there is no capacitor in parallel with input terminals since input is assumed to be voltage source type. Different input and output type is shown in Figure A.1 and Figure A.2.

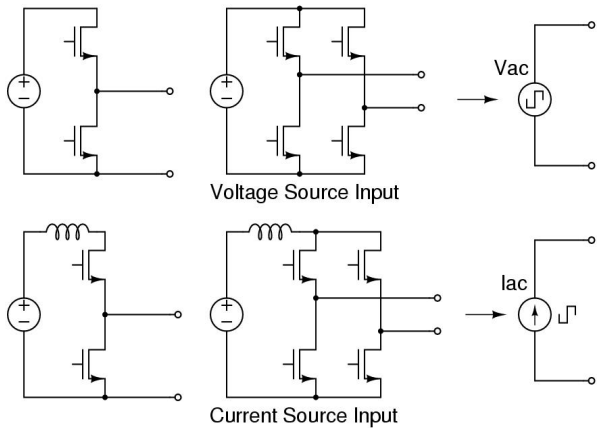

Figure A.1 Input type for DC/DC converter

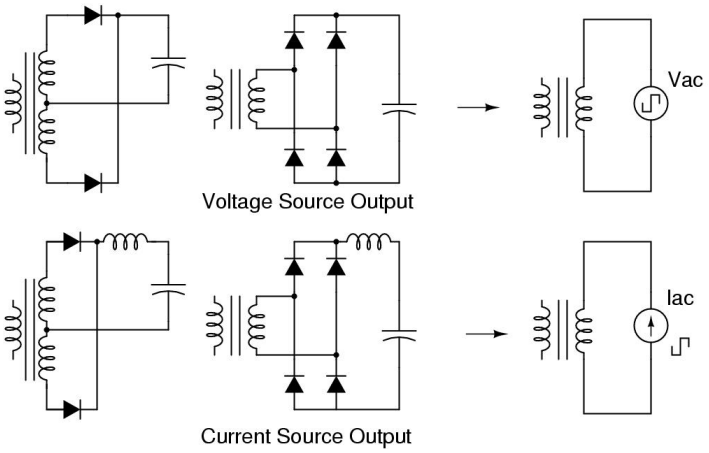

Figure A.2 Input type for DC/DC converter

Third, assume the input is voltage source; output could be voltage source or current source.

A.1. Two resonant components resonant tank

For resonant tank with two resonant components, there are totally eight different type of resonant tank configurations as shown in Figure A.3.

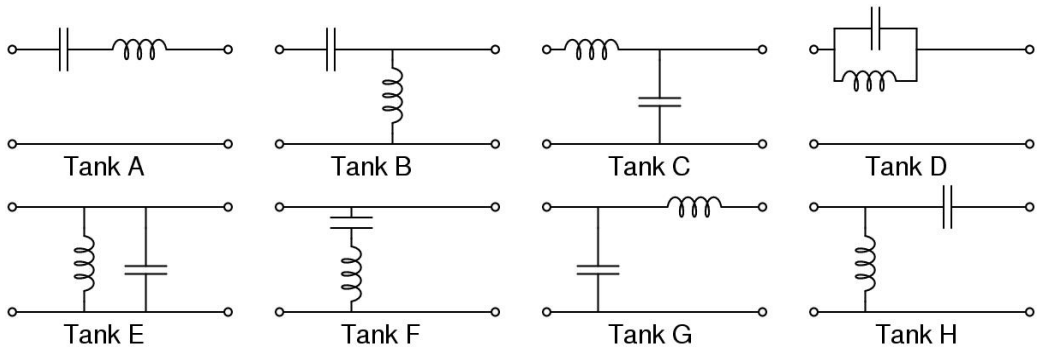

Figure A.3 Two components resonant tanks

In this family, tank A is for series resonant converter. Tank C is for parallel resonant converter. Tank B is another form of parallel resonant converter. Tank E and Tank G requires a current source input, which is not commonly used for this application. Tank F could be used for voltage source input, but it is not meaningful since it cannot regulate power transferred to the load but increase the circulating energy. Tank H could also be applied to voltage source input, but then it is no longer a resonant topology because the resonant inductor will be clamped by input voltage source and never resonant with resonant capacitor. So for two resonant components resonant tank, tank A, B, C and D will be useful.

The characteristics of these four resonant tanks are shown below. We can see that tank B has very similar characteristic with tank C that is widely used as parallel resonant converter.

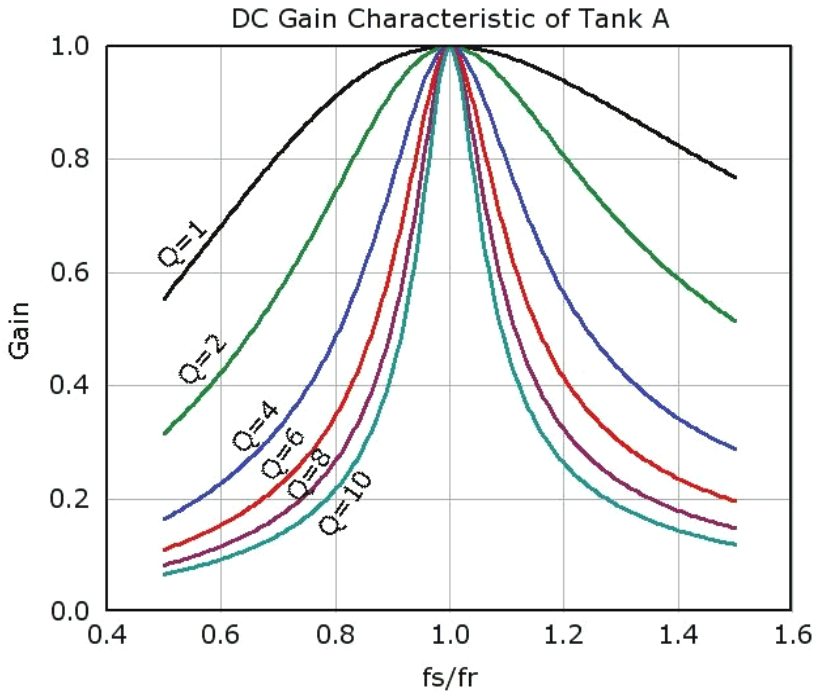

Figure A.4 DC characteristic of two components tank A

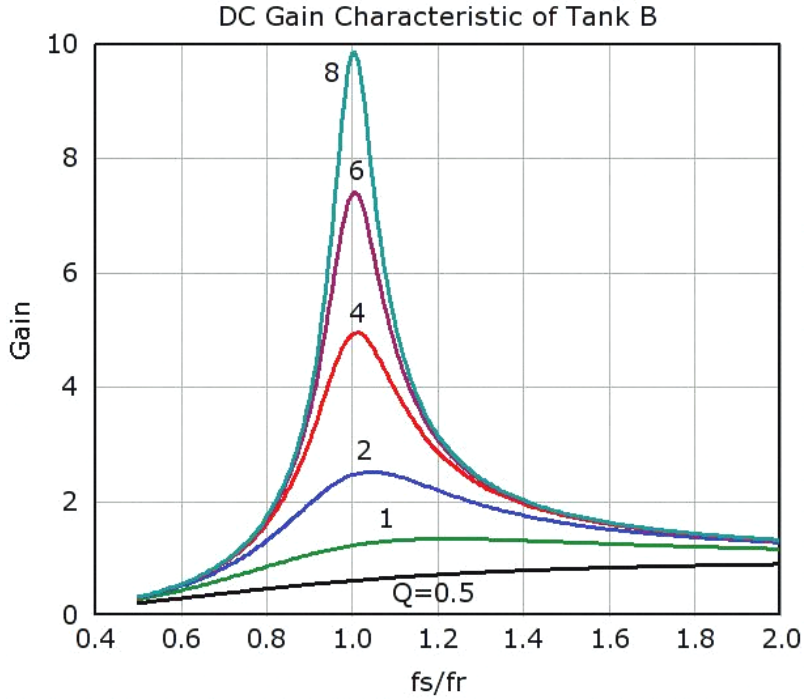

Figure A.5 DC characteristic of two components tank B

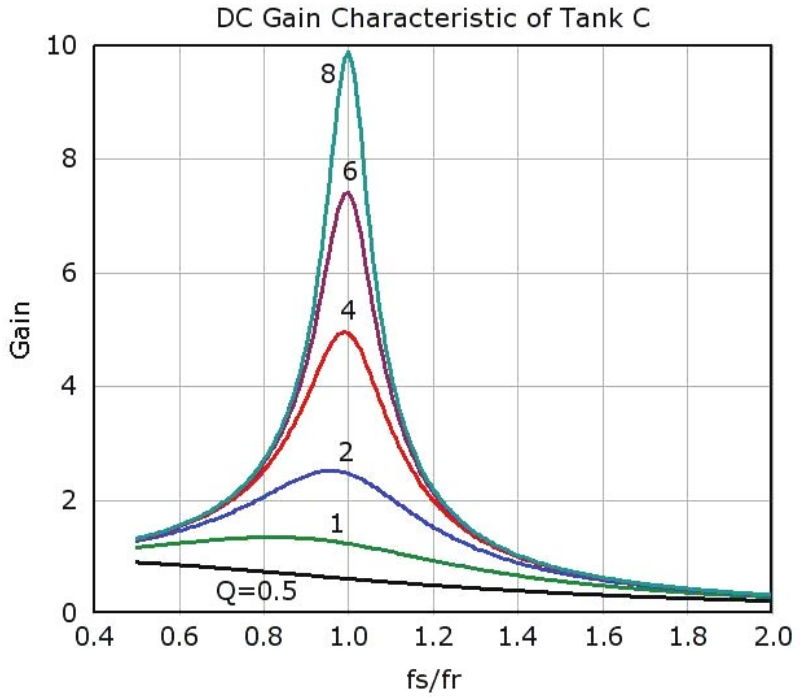

Figure A.6 DC characteristic of two components tank C

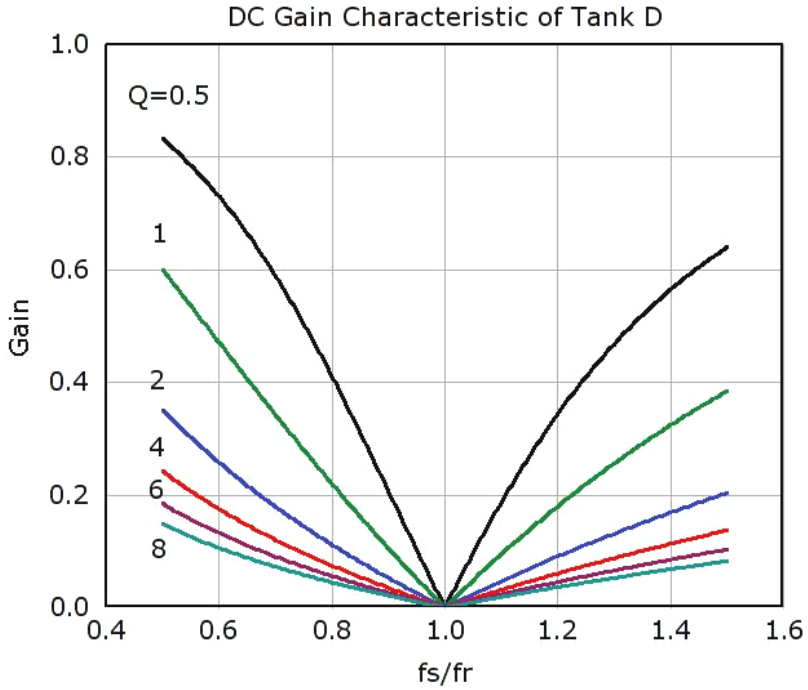

Figure A.7 DC characteristic of two components tank D

A.2. Three resonant components resonant tank

There are many possibilities for three components resonant tank. In this part, they will be listed and classified.

With three components, there are seventeen ways to connect them as shown in Figure A.8.

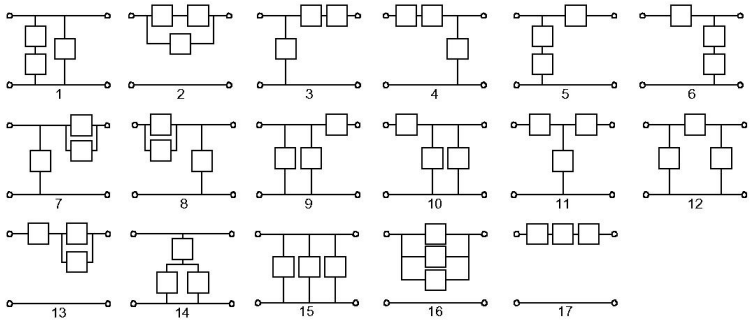

Figure A.8 Components configuration for three components resonant tank

With in these seventeen configurations, 15, 16 and 17 will result to a reduced order since two components could be replaced with one. For the other 14 configurations, with different resonant components, different resonant tank could be constructed. Since we are looking at three components resonant tank, the possible components used could be two Ls and one C or two Cs and one L. Three Ls or three Cs will not result to three components resonant tank and will be eliminated. With fourteen different configurations, there are 36 different resonant tanks as shown below.

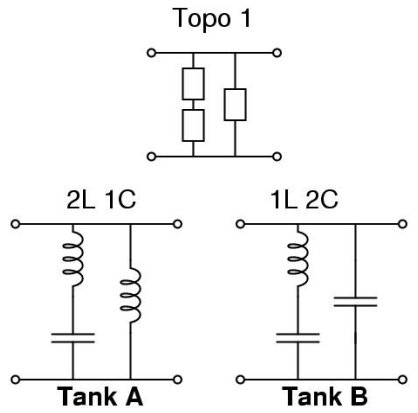

Figure A.9. Resonant tank for components configuration 1

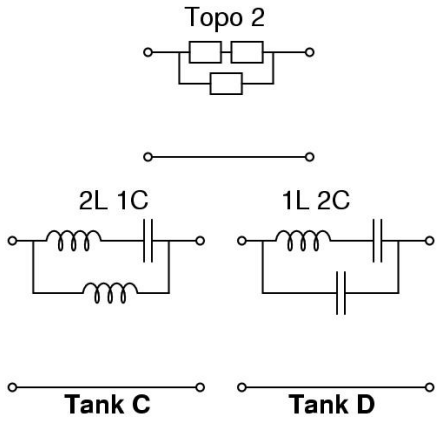

Figure A.10. Resonant tank for components configuration 2

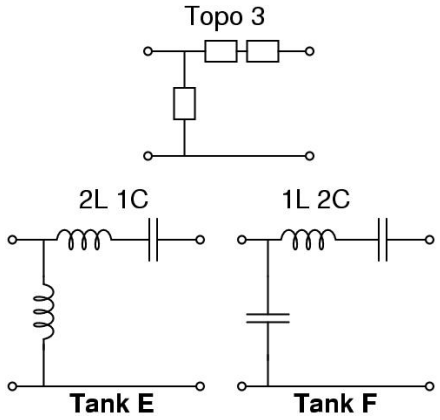

Figure A.11. Resonant tank for components configuration 3

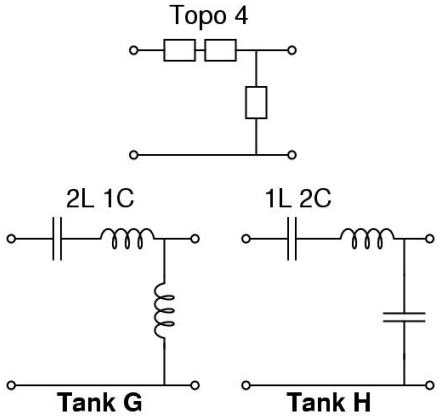

Figure A.12. Resonant tank for components configuration 4

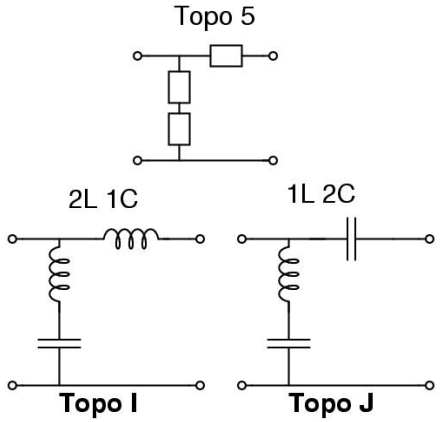

Figure A.13. Resonant tank for components configuration 5

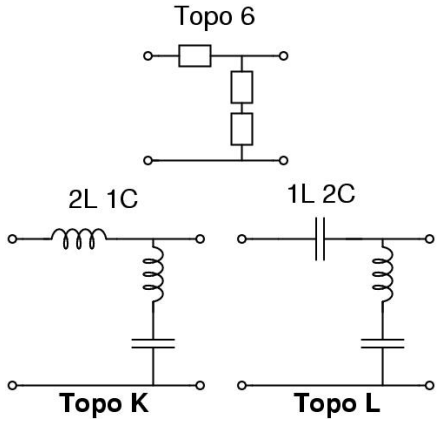

Figure A.14. Resonant tank for components configuration 6

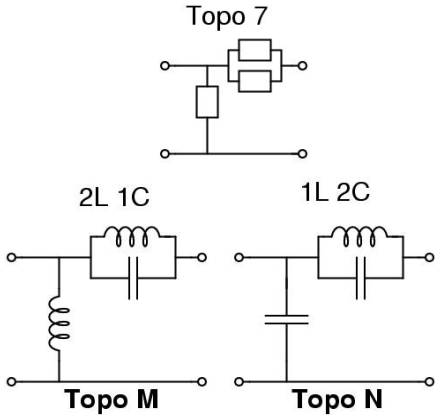

Figure A.15. Resonant tank for components configuration 7

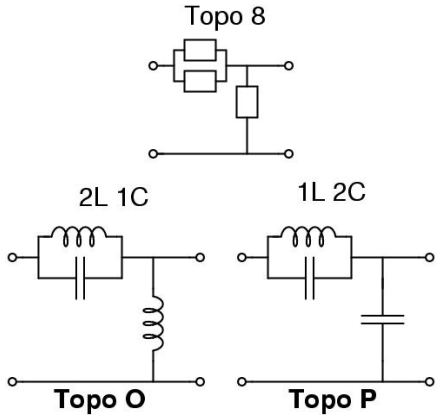

Figure A.16. Resonant tank for components configuration 8

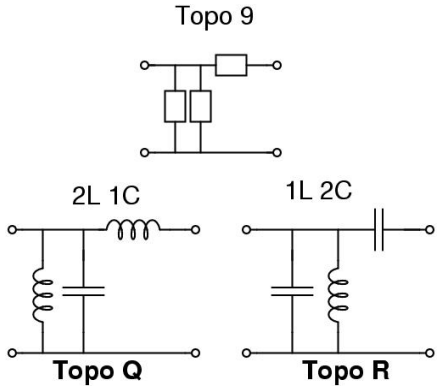

Figure A.17. Resonant tank for components configuration 9

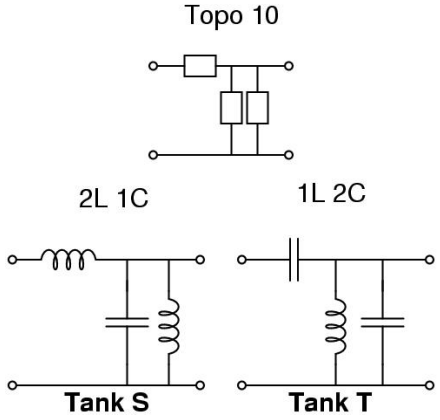

Figure A.18. Resonant tank for components configuration 10

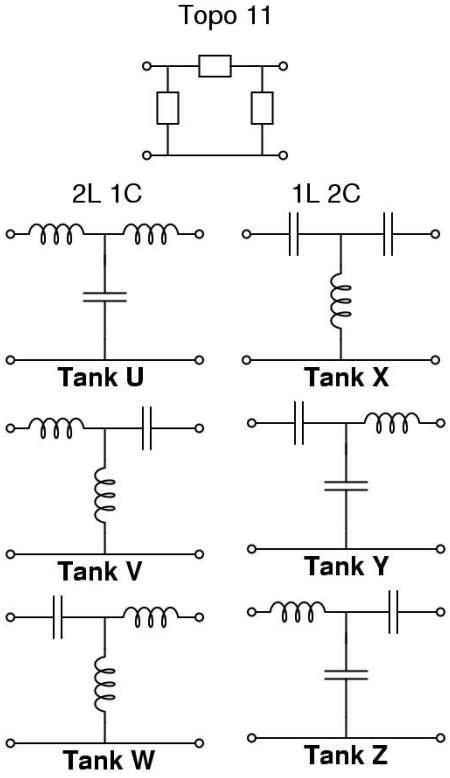

Figure A.19. Resonant tank for components configuration 11

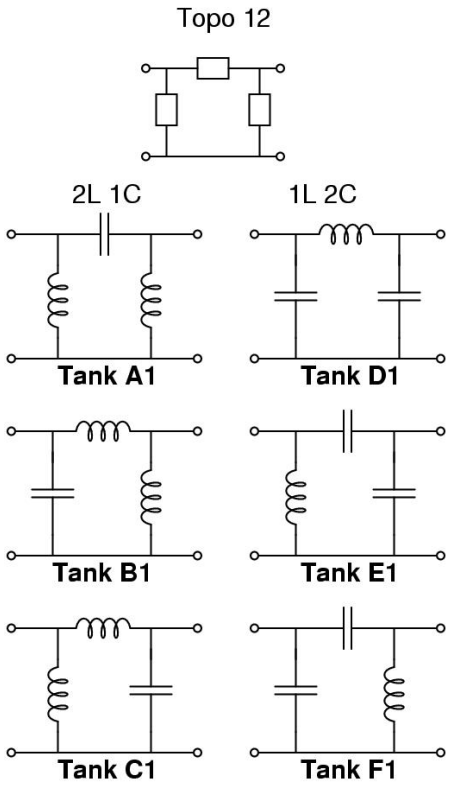

Figure A.20. Resonant tank for components configuration 12

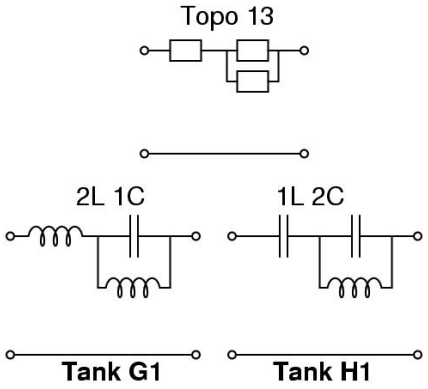

Figure A.21. Resonant tank for components configuration 13

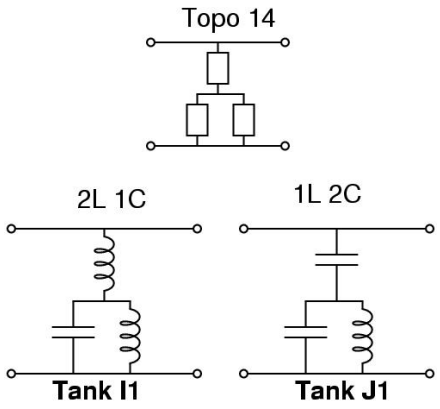

Figure A.22. Resonant tank for components configuration 15

These 36 resonant tanks could be classified in following table. They are classified according to the input source type and output type. For example, for resonant tank A, the input and output are directly connected, so the input and output have to be different type. In the table, it will be list as ITV or VTI, which means the input is current source and output is voltage source or vice versa. Another example is tank Y, since the input of the tank is capacitive, so input has to be current source. The output of the tank is an inductor, so output has to be voltage source. So tank Y could only be applied to ITV.

For these 36 resonant tanks, there are 23 could be used for voltage source input. Next we will continue eliminate some of them. For some resonant tank here, it could not be used to regulate the output. For example, tank A could be used for VTI configuration. Since the resonant components is in parallel with the input, they cannot affect the power transferred to output, which means with this resonant tank, the output could not be regulated with variable frequency control.

For some other resonant tanks, with voltage source configuration, one or more of the resonant components will not participate in controlling output power. For example, in tank I, the series resonant branch is in parallel with input. The current through this branch will not have effect on output power. So it will not behave as three components resonant converter anymore.

Table A-1 Classification of three components resonant tanks

Tank	*VTV*	*VTI*	*ITV*	*ITI*	*Topo*		*VTV*	*VTI*	*ITV*	*ITI*	*Topo*
A		V	I		1	S		V	I		10
B			I	I	1	T			I	I	10
C	V				2	U	V				11
D		V	I		2	V	V		I		11
E	V				3	W	V				11
F			I		3	X		V	I		11
G	V				4	Y					11
H		V			4	Z		V			11
I	V				5	A1		V			12
J		V	I		5	B1			I		12
K	V				6	C1		V			12
L		V	I		6	D1			I		12
M		V	I		7	E1			I		12
N			I	I	7	F1			I	I	12
O		V	I		8	G1	V		I		13
P			I	I	8	H1		V	I	I	13
Q			I		9	I1		V	I		14
R			I	I	9	J1			I	I	14
Total							9	14	23	9	

Base on above rules, tank A, E, I, J, M, A1, C1 and I1 will be eliminated. So the resonant tank could be used for voltage source input are listed as following:

Table A-2 Three components resonant tanks with voltage source input

Tank	*VTV*	*VTI*	*Topo*
C	V		2
D		V	2
G	V		4
H		V	4
K	V		6
L		V	6
O		V	8
S		V	10
U	V		11
V		V	11
W	V		11
X		V	11
Z		V	11
G1	V		13
H1		V	13
	6	9	

Next the DC characteristic of each resonant tank will be derived.

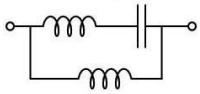

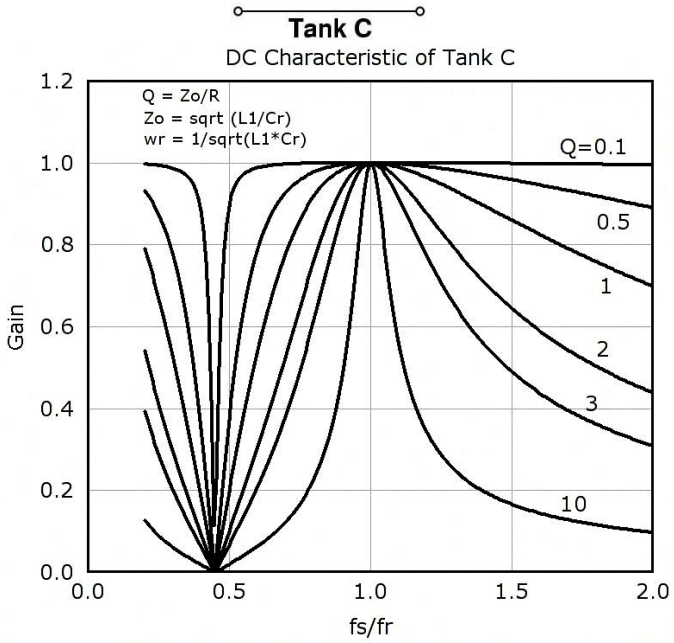

Figure A.23. DC characteristic of tank C

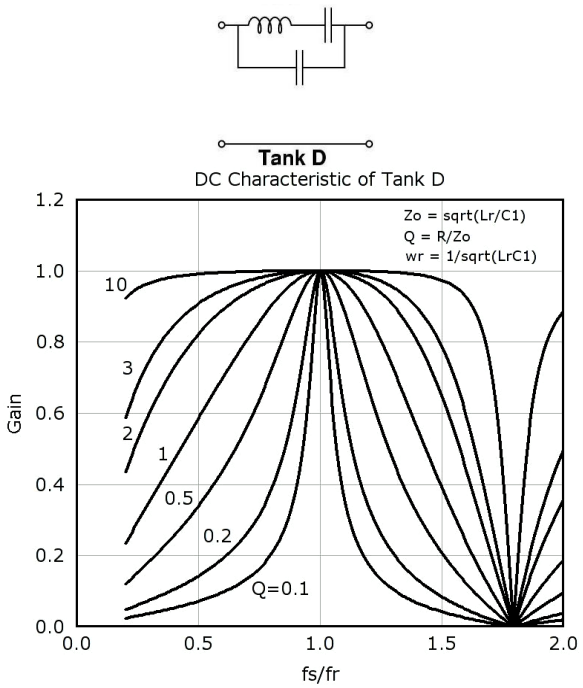

Figure A.24. DC characteristic of tank D

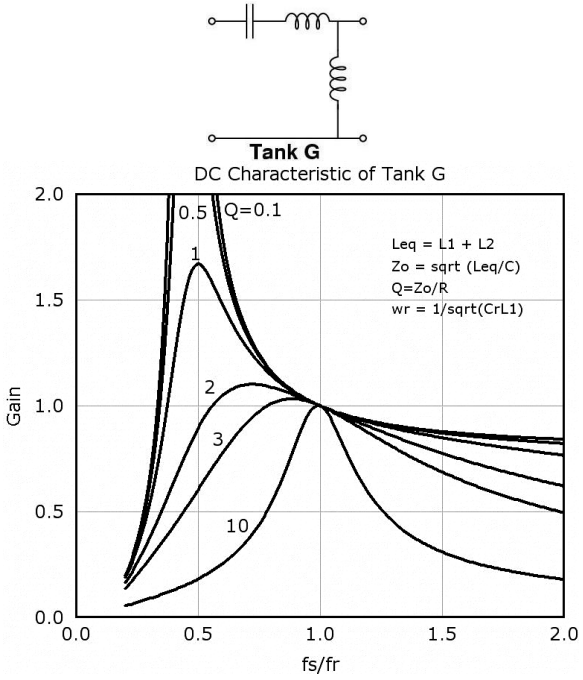

Figure A.25. DC characteristic of tank G

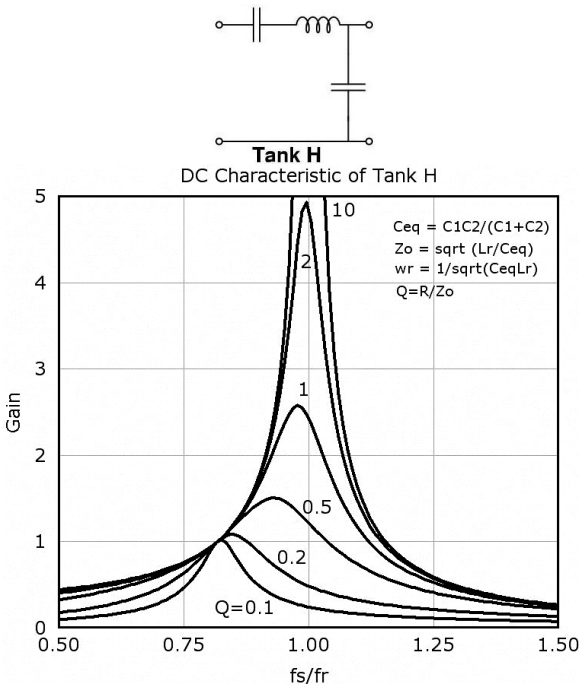

Figure A.26. DC characteristic of tank H

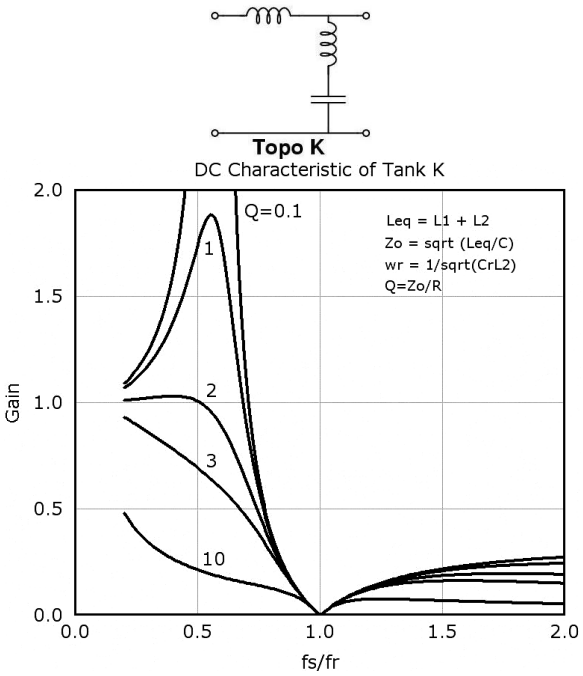

Figure A.27. DC characteristic of tank K

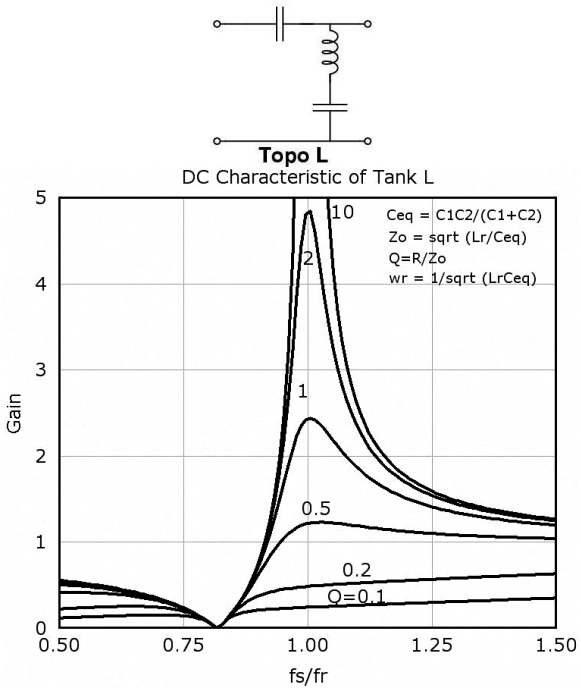

Figure A.28. DC characteristic of tank L

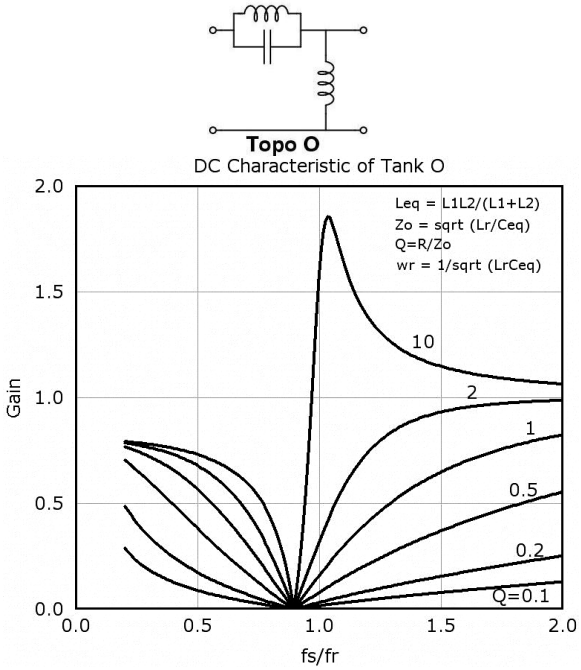

Figure A.29. DC characteristic of tank O

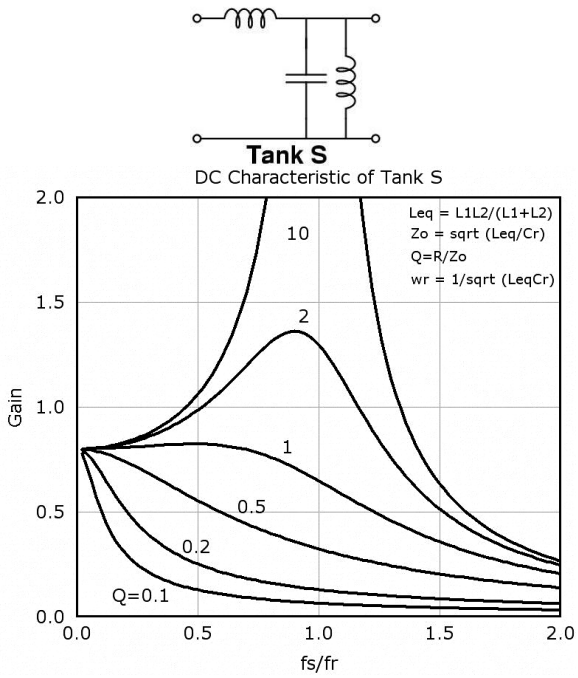

Figure A.30. DC characteristic of tank S

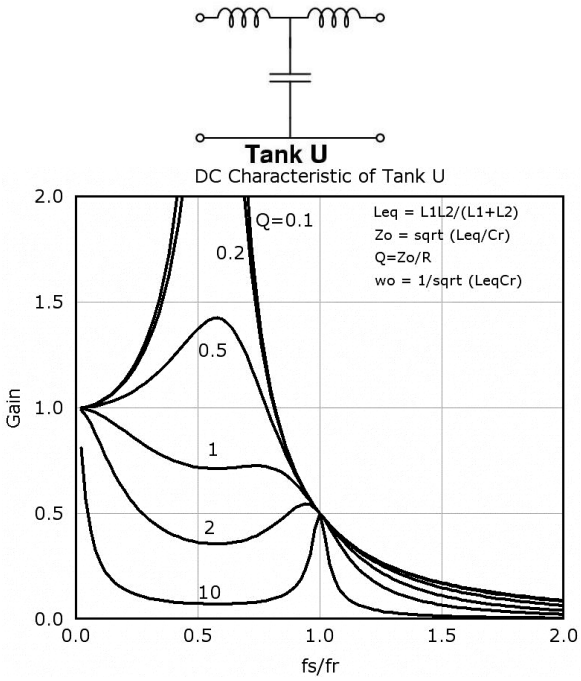

Figure A.31. DC characteristic of tank U

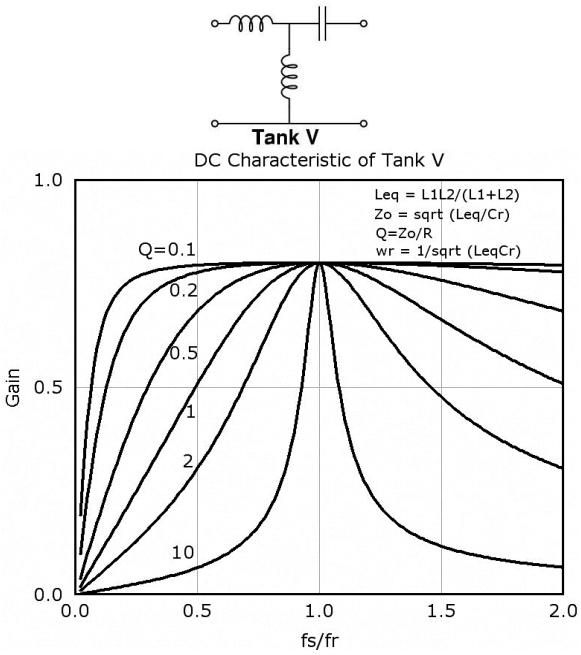

Figure A.32. DC characteristic of tank V

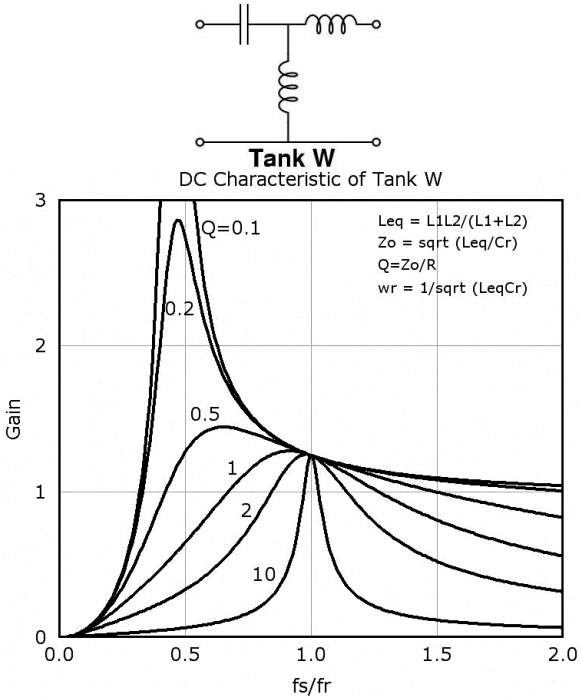

Figure A.33. DC characteristic of tank W

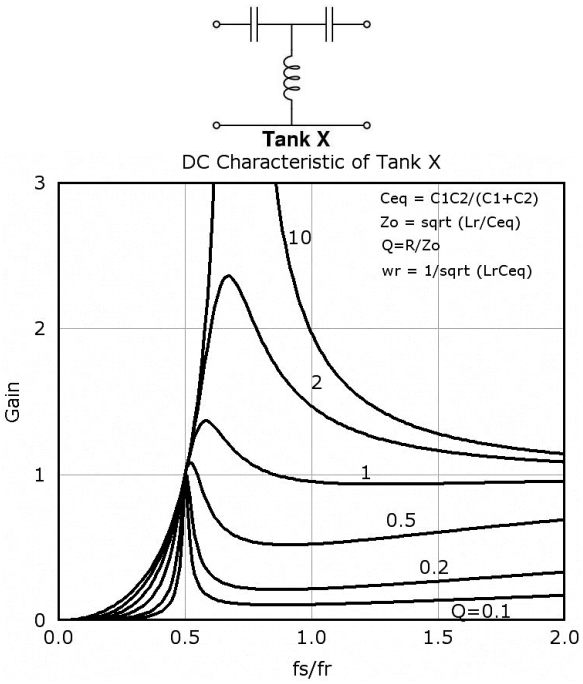

Figure A.34. DC characteristic of tank X

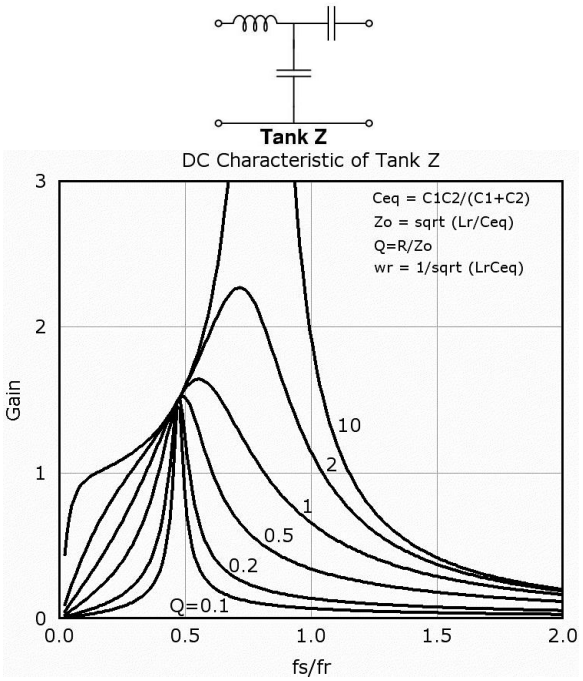

Figure A.35. DC characteristic of tank Z

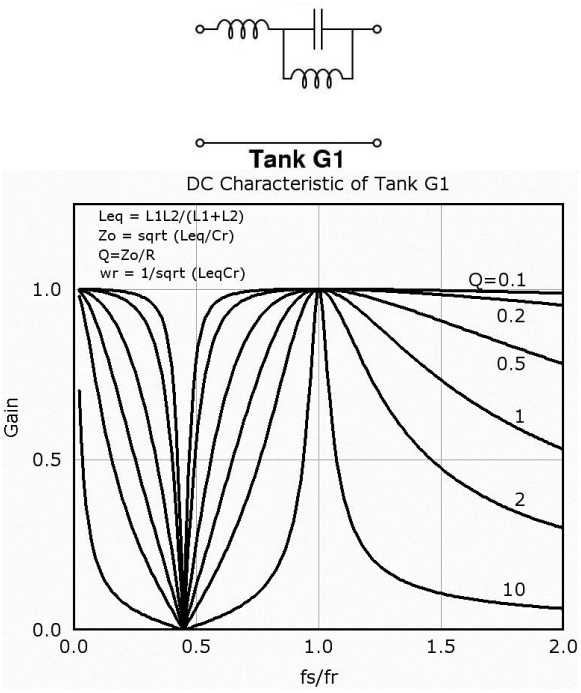

Figure A.36. DC characteristic of tank G1

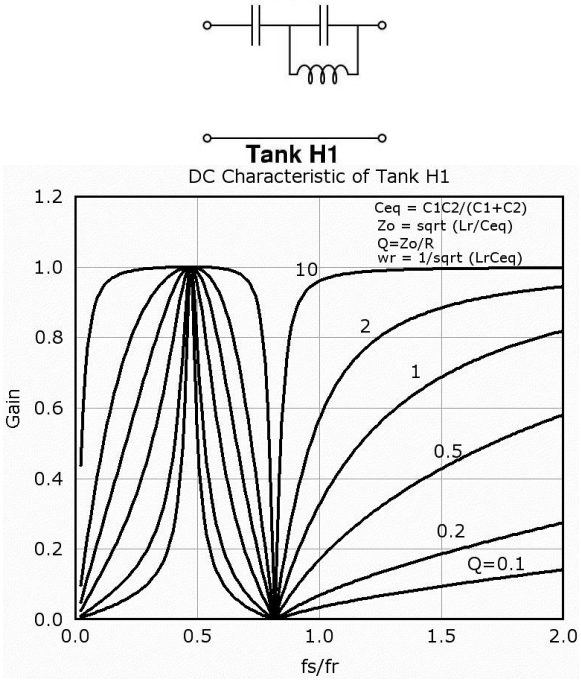

Figure A.37. DC characteristic of tank H1

In above resonant tanks, tank H, X and Z have similar characteristic as traditional called LCC resonant converter. For resonant tank G, U and W, they have the characteristic of LLC resonant converter.

Appendix B.

Operation modes and DC analysis of LLC resonant converter

In this part, different operation modes of LLC resonant converter will be discussed.

LLC resonant converter, as a three resonant components resonant converter, has many different operating modes. It is a multi resonant converter. During one switching cycle, the resonant tank configuration changes. With different load condition, discontinuous conduction mode could happen. In this part, different operating modes in different operating region and load condition will be listed.

From the DC characteristic of LLC resonant converter, the operating of LLC resonant converter could be divided into three regions as shown in Figure B.1. As discussed in chapter 3, region 1 and region 2 are ZVS regions, which are preferred for high frequency operation. In region 3, the converter is working under ZCS. For this converter, preferred operating regions are region 1 and region 2 in order to achieve ZVS.

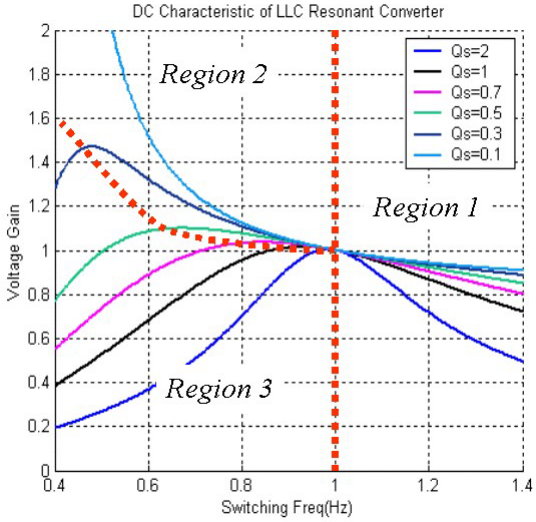

Figure B.1 DC characteristic of LLC resonant converter

B.1. Operating modes of LLC resonant converter in Region 1

In region 1, the converter works very similar as a SRC. But because of the impact of Lm, there are some new operation modes for LLC resonant converter. In this region, there are three different operating modes as load changes.

Operating mode 1 in region 1

This mode of operation is same as a SRC. Resonant components Lr and Cr act as the series resonant tank. During whole switching cycle, Lm is clamped by output voltage and never participates in the resonant process. This mode also could be called as continuous conduction mode since the output current is always continuous.

In this operation mode, Lm just acts as a passive load of series resonant tank of Lr and Cr. The operating waveforms are shown in Figure B.2.

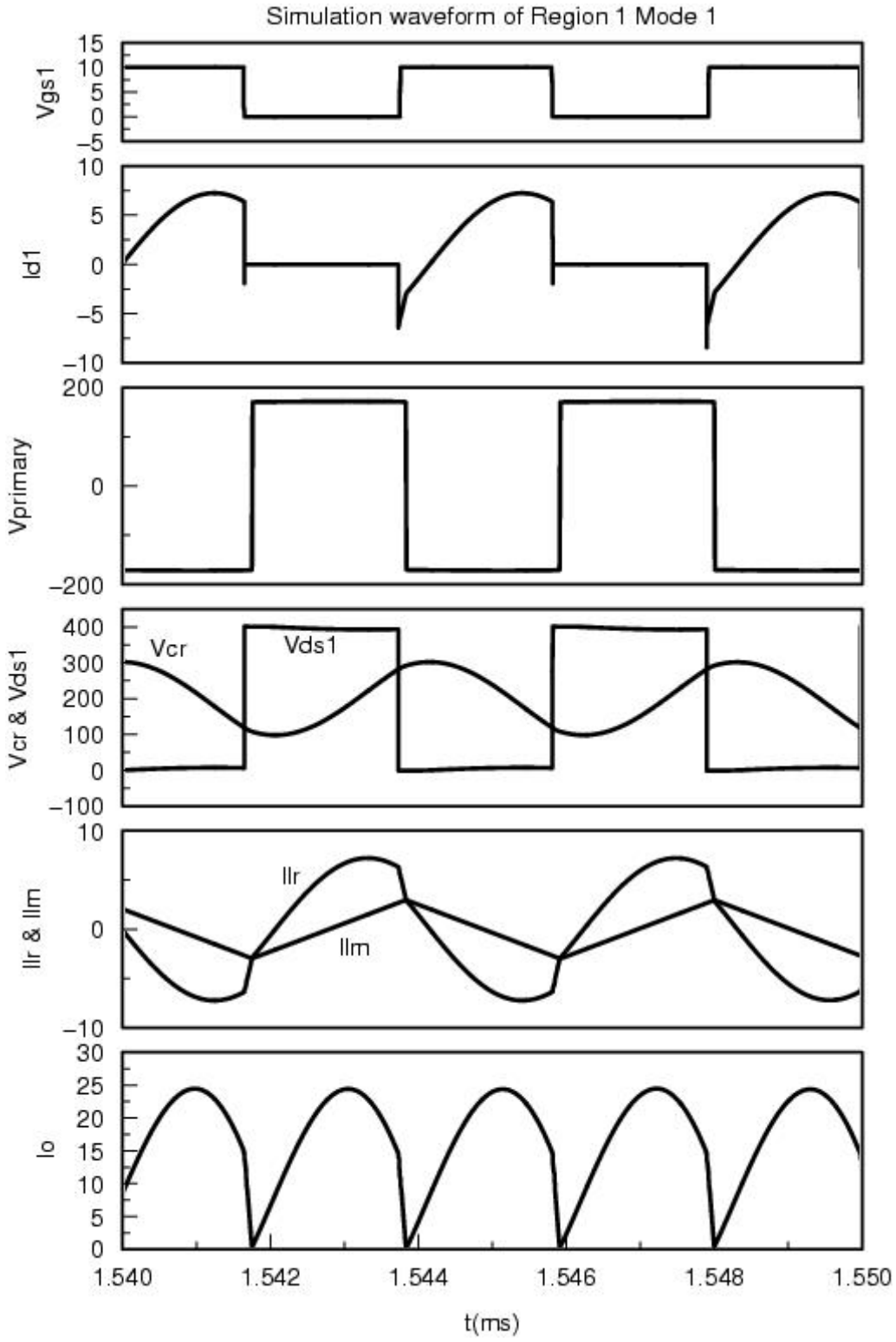

Figure B.2 Waveform of operation mode 1 in region 1 for LLC resonant converter'

Operating mode 2 in region 1

As load becomes lighter, the converter will work into mode 2. The different of mode 2 and mode 1 is that after primary switches been switched, there will have a time period during which the secondary current is zero, or discontinuous conduction mode. During this dead time, primary current is clamped to the Lm current, the resonant tank will be consisted with Cr and Lm in series with Lr.

This mode happens when following condition is met:

$$(V_{IN} + V_{Cr}) \cdot \frac{Lm}{Lm + Lr} < Vo \cdot n$$

When above condition is met, when primary switches switched, the voltage apply to the Lm is the left of above equation. If this voltage is lower than the output voltage reflected to the primary side, the output diodes would not conduct, only after Lm current continuous charge Cr so that above condition is broken, the output filter diodes begin to conduct. Then Lm will be clamped to output voltage and no longer resonant with Cr.

During this mode, Lm not only acts as the load of SRC, it also participate in the resonant with Cr. For SRC, there is no DCM in this region.

The operating waveforms are shown in Figure B.3. Because of existence of Lm, there are more circulating current for LLC at light load compared with SRC. But the benefit is ZVS is ensured at light load condition.

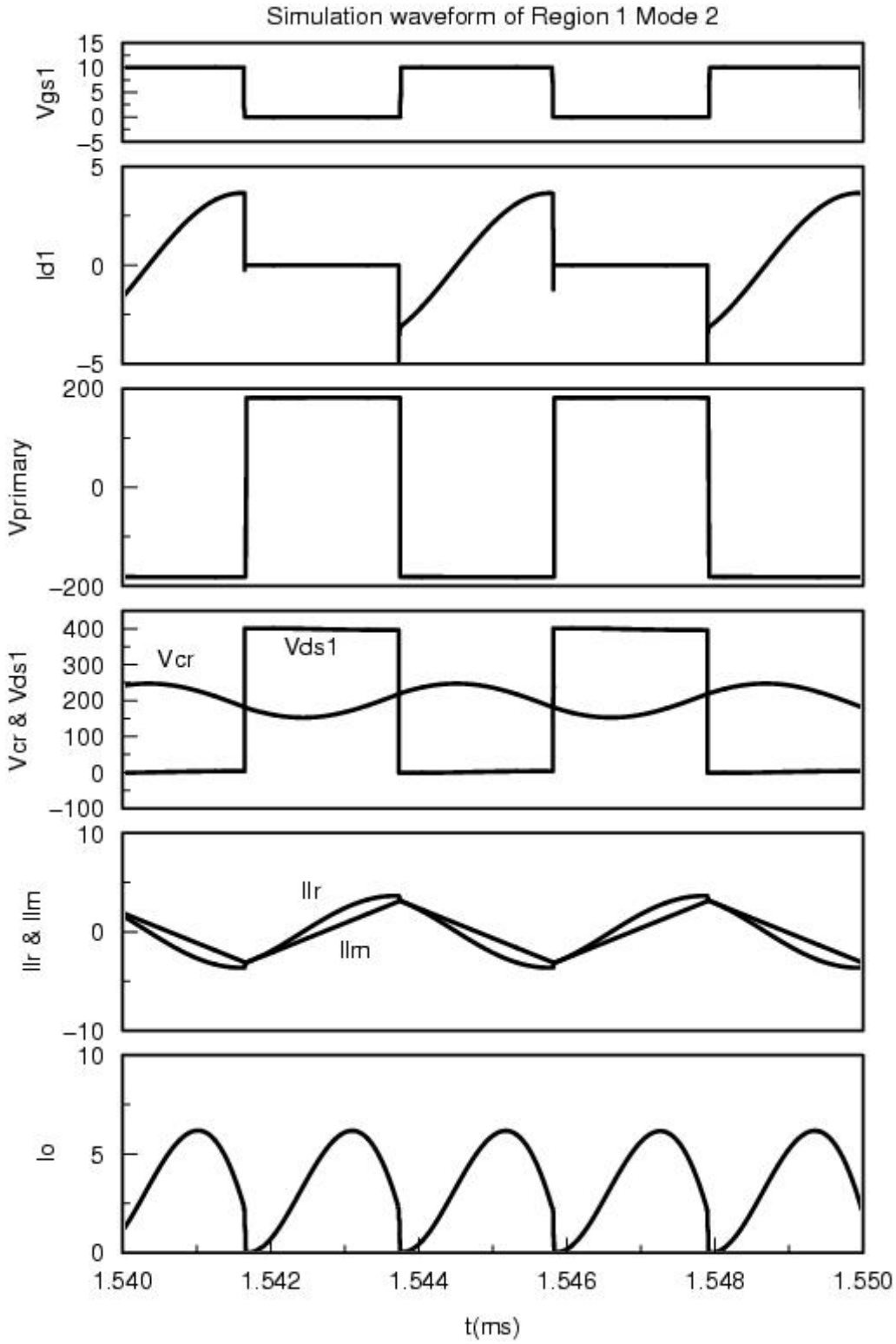

Figure B.3 Waveform of operation mode 2 in region 1 for LLC resonant converter'

Operating mode 3 in region 1

If load continuous reduce, the converter will works into mode 3. This mode looks very similar to mode 2. But in fact, there are two kinds of discontinuous conduction modes in this operating mode. First DCM happens after the primary switches been switched as in Mode 2. But during the switching cycle, another discontinuous mode happens. From the Lr and Lm current, it can be seen that Lr current resonant and then clamped to Lm current before the switching action of primary switch. This will introduce a zero current period before primary switch action.

The operating waveforms of this operating mode are shown in Figure B.4. From the waveforms, it can be seen that ZVS is still achieved because of Lm. This is the major benefit of LLC converter been discussed before. With Lm, the ZVS at light load could be maintained. Also, light load regulation is easier since Lm is always presents as the load of the SRC.

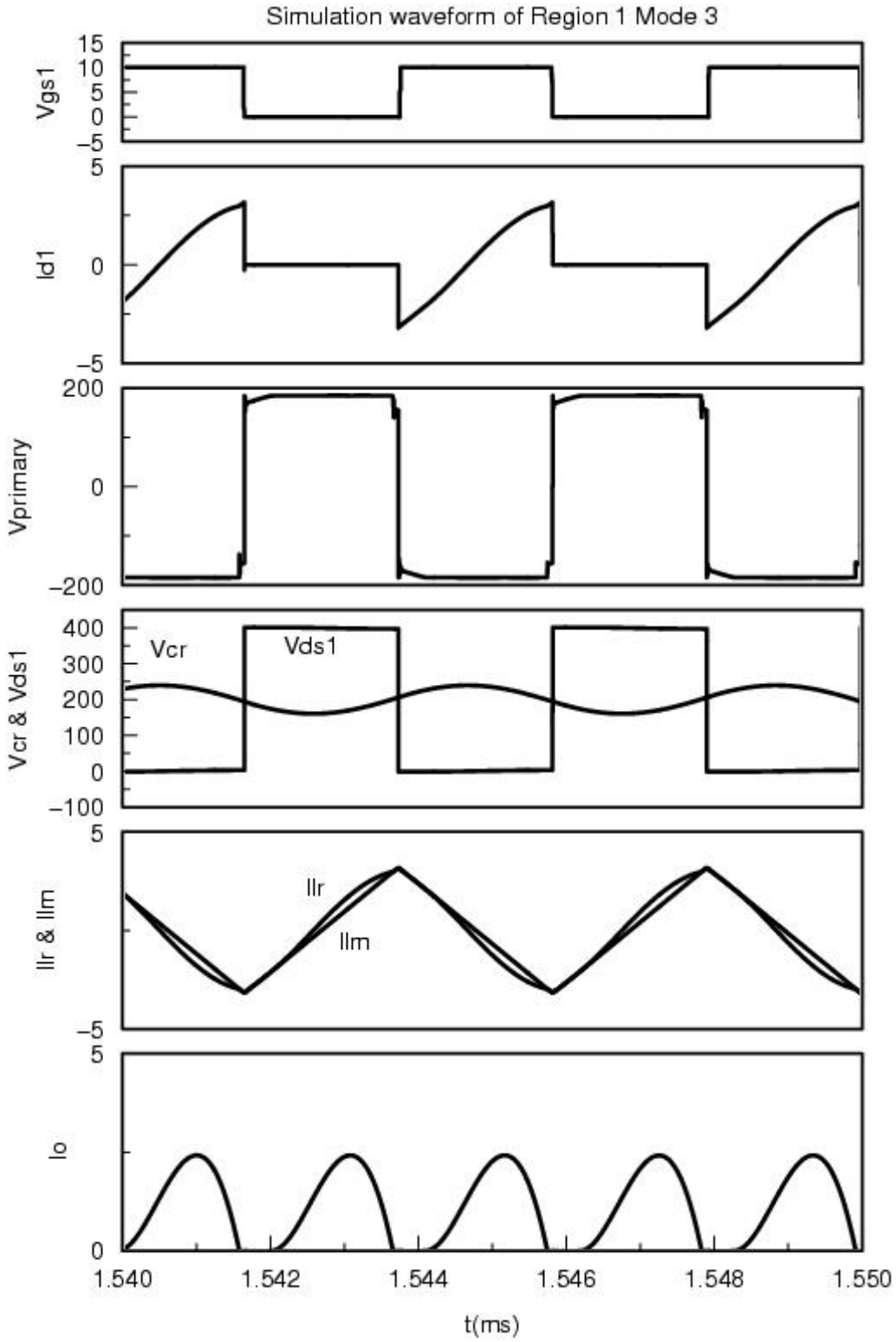

Figure B.4 Waveform of operation mode 3 in region 1 for LLC resonant converter'

B.2. Operating modes of LLC resonant converter in Region 2

This region is a very interesting region. Traditional SRC will work into ZCS when working in this region, so there is no region 2 for SRC. For LLC, with the presents of Lm, even when switching frequency is lower than resonant frequency of Lr and Cr, the converter could still work in ZVS condition with higher gain.

In this region, also exist three operating modes with different load conditions.

Operating mode 1 in region 2

This is the designed operating mode for LLC resonant converter at full load. The waveforms of this operating mode are shown in Figure B.5. The major characteristic of this operating mode is the two different resonant time periods. First, when primary switches switched, Lr and Cr will resonant. During this time period, Lm is clamped by output voltage and is linearly charged. When Lr current resonant back to the same level as Lm current, second resonant happens, which is the resonant between Cr and Lm in series with Lr. This resonance will last till the primary switches been switched again. During second resonant time period, the output current keeps zero. So the output current in this operation mode is discontinuous. As seen in the waveforms, ZVS is achieved with Lm current. This gives us freedom to choose desired turn off current to achieve ZVS while with low turn off loss.

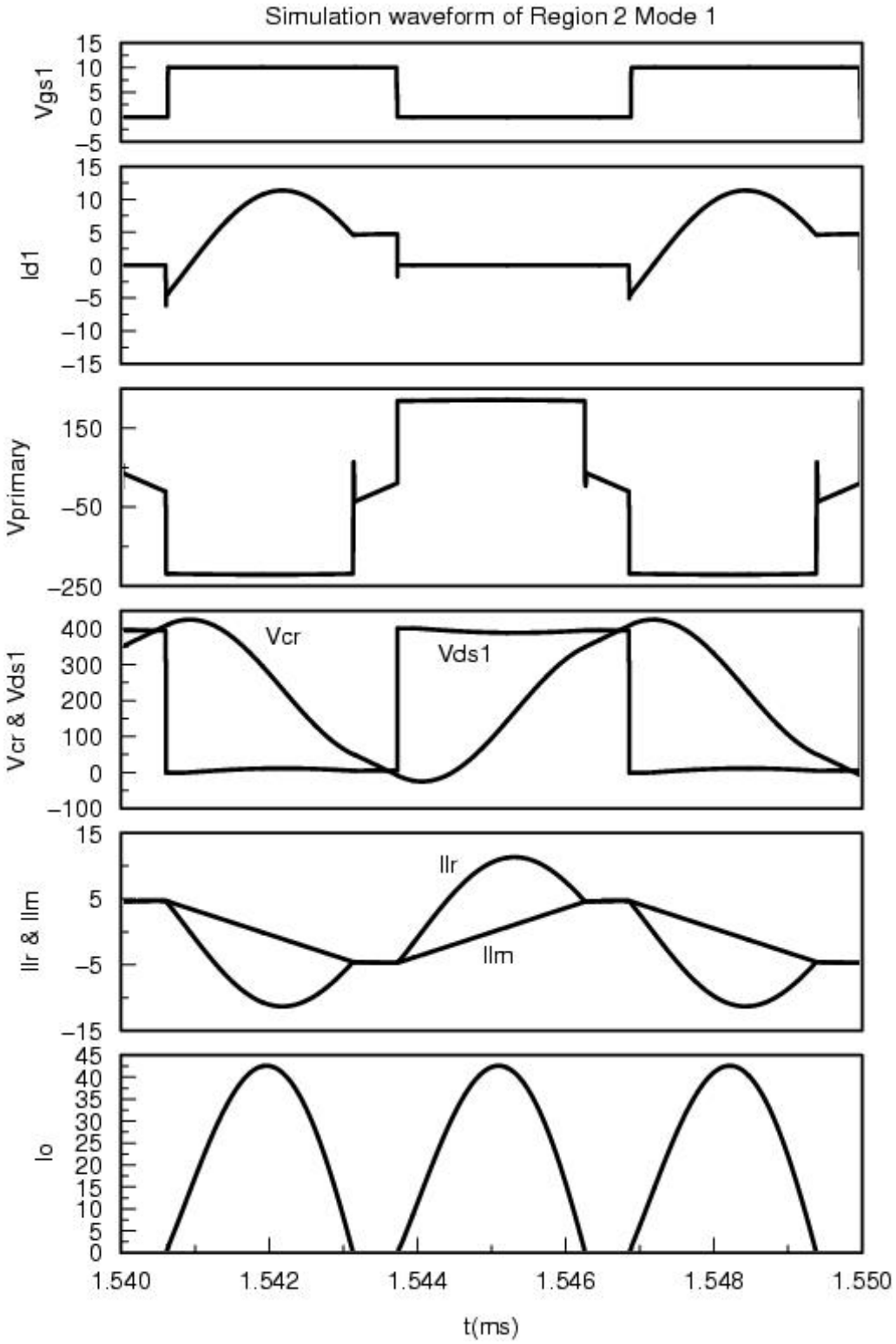

Figure B.5 Waveform of operation mode 1 in region 2 for LLC resonant converter'

Operating mode 2 in region 2

In mode 1, the output current is already discontinuous. As load becomes lighter, another discontinuous mode will exist.

This discontinuous mode is very similar to operating mode 2 in region 1. When load becomes lighter, the voltage on resonant capacitor Cr will be lower when primary switches switched. If following condition is satisfied, then the secondary diodes will not conduct. This will introduce a zero current period on the output current after primary switching action.

$$(V_{IN} + V_{Cr}) \cdot \frac{Lm}{Lm + Lr} < Vo \cdot n$$

As seen in the waveform, the energy flows back and forth from input, which means most of the current are circulating in this mode. Although this causes higher conduction loss at light load, it makes the converter operating with ZVS at very light load. This circulating current is controllable through careful design of Lm.

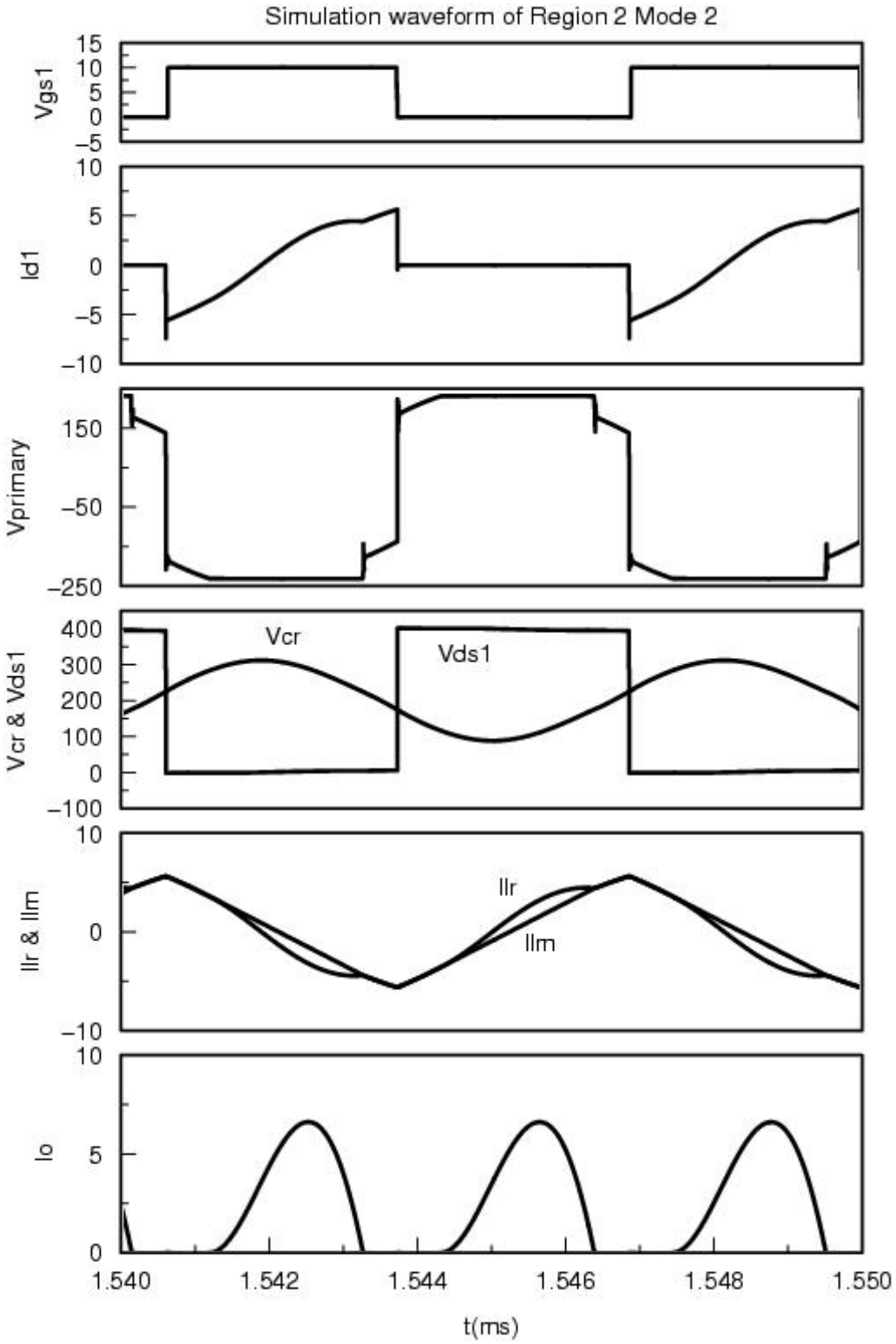

Figure B.6 Waveform of operation mode 2 in region 2 for LLC resonant converter'

Operating mode 3 in region 2

This is a mode in region 2 happens when the load is too heavy. In mode 1, two resonant periods exist in half switching cycle. In this mode, three modes will exist in half switching cycle.

First two time intervals are the same as in mode 1. If load is too heavy, resonant capacitor Cr voltage ripple will increase. If Vcr is high enough to met following equation, the third resonant period will happen:

$$(V_{Cr} - V_{in}) \cdot \frac{Lm}{Lm + Lr} < V_O \cdot n$$

As shown in the waveforms in Figure B.7, after Lr current resonant back to save level of Lm current, instead of clamped by Lm current, it will resonant to the other direction. This is because of too high energy is stored in resonant capacitor Cr that its voltage is high enough to make secondary diodes conduct. With this mode, the switch turn off current will be less than Lm current. The risk is that the energy is not enough for ZVS. Also, if Lr current resonant to negative, the converter will work into region 3.

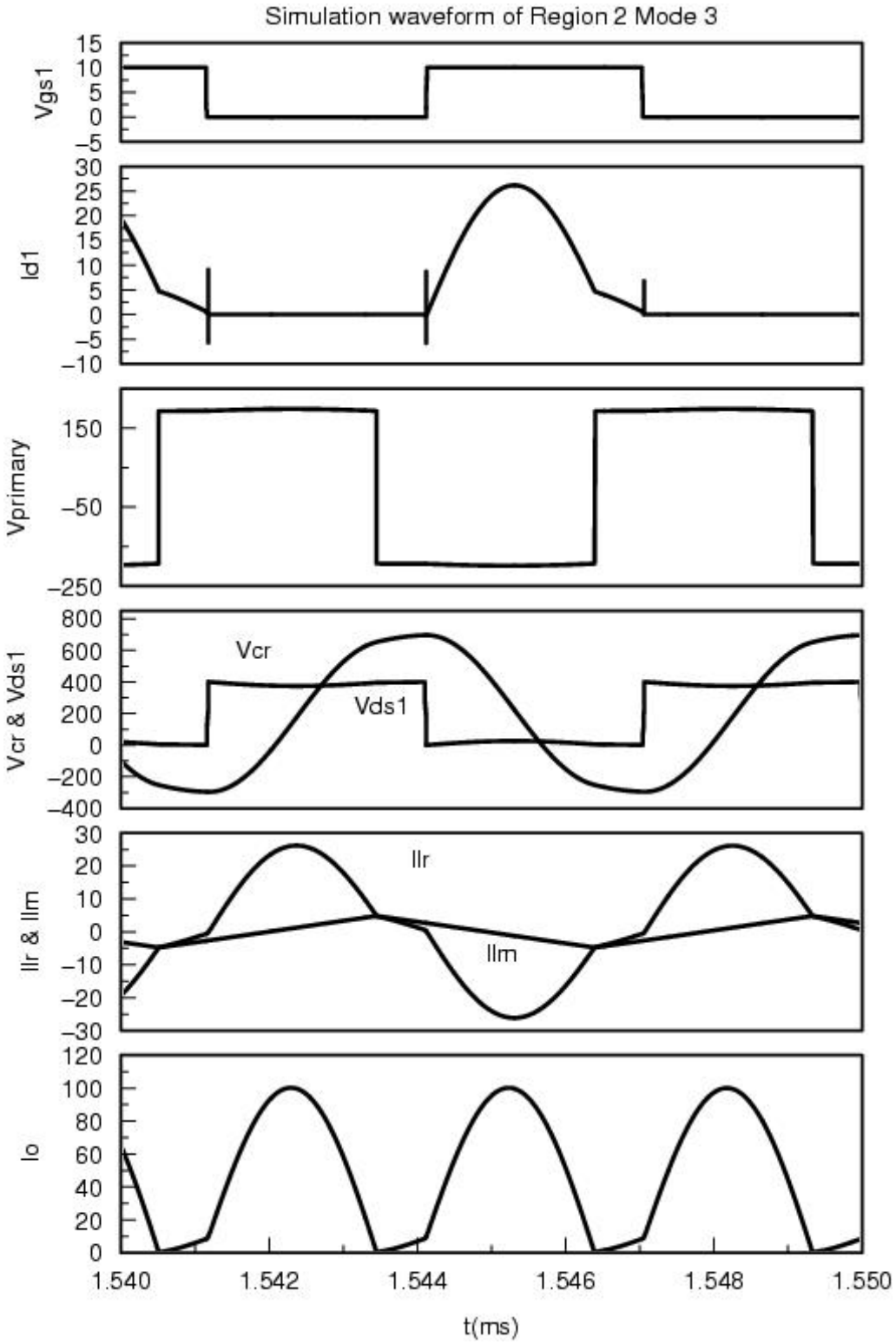

Figure B.7 Waveform of operation mode 3 in region 2 for LLC resonant converter'

B.3. Operating modes of LLC resonant converter in Region 3

Region 3 is a ZCS region. In this region, the DC gain characteristic has positive slope. As seen from the waveforms in Figure B.8, switch is turned off after its body diode begins to conduct. This is not a preferred operating mode for MOSFET. In the design, this mode should be prevented.

These different operating modes will happen during the operation of LLC resonant converter. For the discontinuous operating modes, they will not affect the ZVS capability of the converter because of presents of Lm. During heavy load in region 2, the converter will come into ZCS. As discussed in over load protection, applying clamped LLC resonant topology could prevent this.

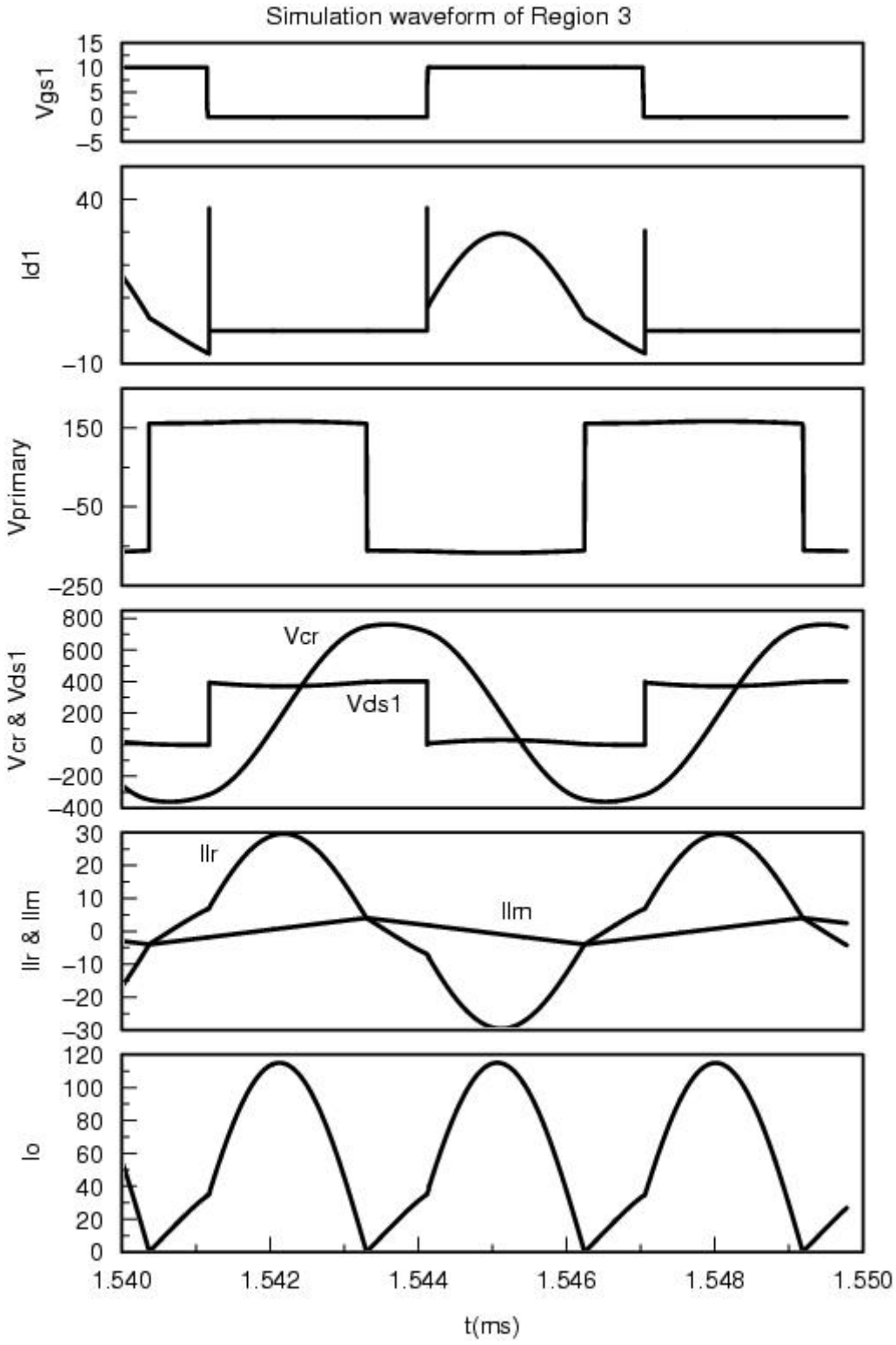

Figure B.8 Waveform in region 3 for LLC resonant converter

B.4. DC analysis of LLC resonant converter

In this part, two aspects will be addressed. First is the DC characteristic. DC characteristic is the most important information for the converter design. With DC characteristic, the parameters could be chosen; the design trade offs can be made. For LLC resonant converter, the DC characteristic will draw the relationship between voltage gain and switching frequency for different load condition.

Traditionally, fundamental element simplification method was used to analysis the DC characteristic of resonant converter. The fundamental element simplification method assume only the fundamental components of switching frequency is transferring energy. With this assumption, the nonlinear part of the converter like switches, Diode Bridge could be replaced with linear components. The simplified converter will be a linear network to analysis. So with this method, the DC characteristic could be derived very easily. And the result will be a close form equation, which is easy to use.

For LLC resonant converter, the simplification could be done as shown in Figure B.9.

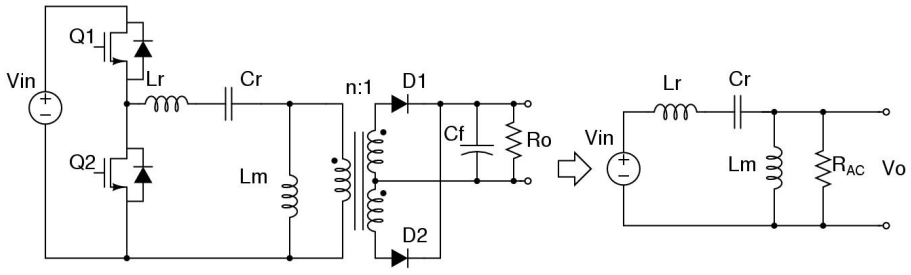

Figure B.9 Simplified topology with fundamental component assumption

With this simplified circuit model, the DC characteristic could be get as:

$$\frac{Vo}{Vin} = \frac{j \cdot \omega_n \cdot Q_l}{j \cdot \omega_n (Q_l + 1 - \frac{1}{\omega_n^{\,2}}) + Q_l (1 - \omega_n^{\,2}) Q_s \cdot \frac{8}{\pi^2}}$$

ω_n : Normalized switching frequency

$\mathrm{Zo}: \sqrt{\frac{\mathrm{Lr}}{\mathrm{Cr}}}$

Q_l: : Ratio of two resonant inductance $\frac{\mathrm{Lm}}{\mathrm{Lr}}$

R_{AC}: Equivalent Load Resistance $\frac{8}{\pi^2} Ro \cdot n^2$

Q_s: $\frac{\mathrm{Zo}}{\mathrm{Ro}}$

For this method, there are some limitations. Because this method is a simplified method, error will be generated with different operating point. When the current waveform is not sinusoidal and contains more high order harmonic, this method will generate high error. To evaluate this error, a more accurate DC characteristic is needed. Here simulation is used to derive the accurate DC gain characteristic. A time domain switch circuit model is built in simulation software. By changing the switching frequency and load condition, a output voltage can be get for each point. Sweep load and switching frequency, an accurate DC characteristic is got. The results of these two methods are shown in following figures. And the error is also shown.

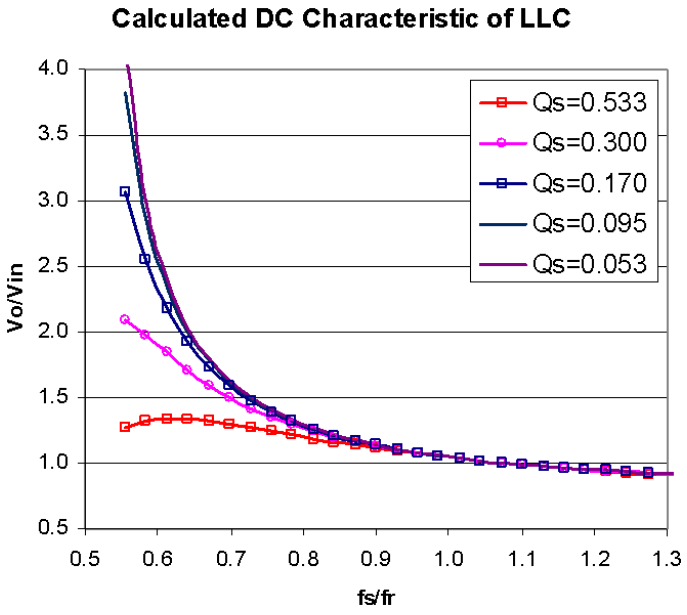

Figure B.10 DC characteristic from simplified model

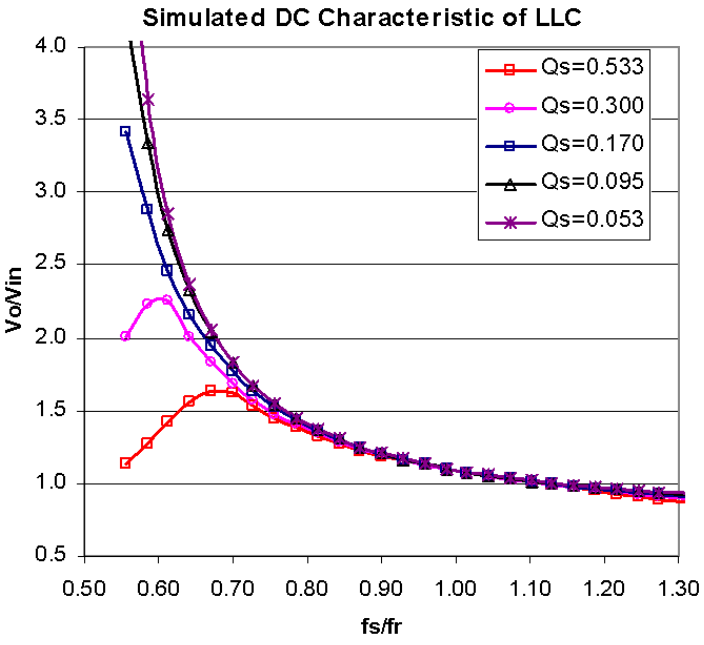

Figure B.11 DC characteristic from simulation method

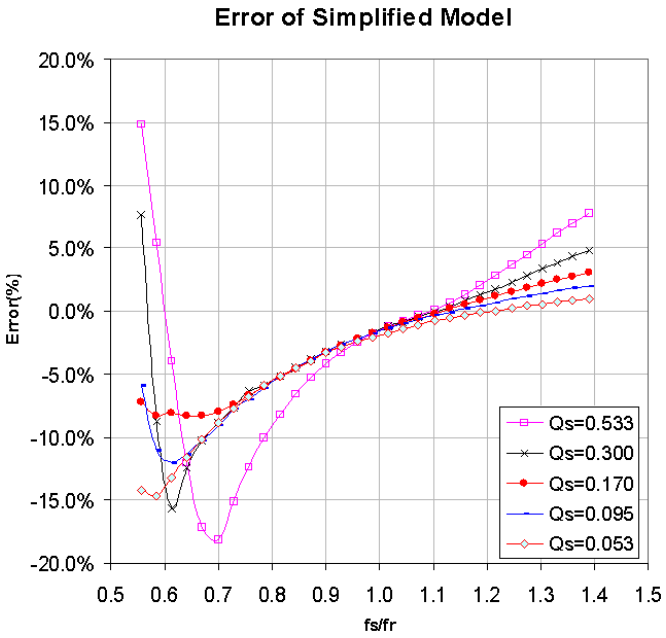

Figure B.12 Error of simplified circuit model

From the error it can be seen that, when the switching frequency equals to the resonant frequency, there is no error. When the switching frequency is moving away from resonant frequency, the error will be high. This can be understood from waveform also; when the circuit works at resonant frequency, the current waveform is exactly sinusoidal, so simplified model doesn't have any error. When switching frequency is away from resonant frequency, high order harmonic content will increase, which will affect the accuracy of the simplified model.

For the design of LLC resonant converter, the trade offs are more affected by operating point with maximum gain. With simplified model, large error will be introduced. Simulation gives accurate results; the issue is that it is time consuming. A better method is to combine these two methods. During primary

design, use simplified model to get a range. To optimize the design, simulation method is preferred to get a better design.

Appendix C.

Small signal characteristic of SRC converter

C.1. Small signal characteristic of SRC

The circuit parameters for SRC used in the simulation are shown in Figure C.1. The small signal characteristic get from simulation are shown in Figure C.2.

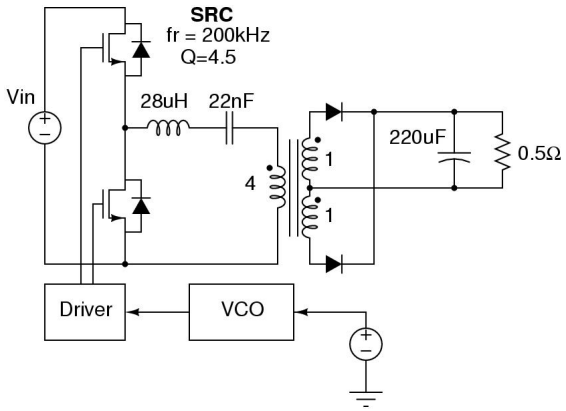

Figure C.1 SRC circuit for small signal analysis

In the graph, the x-axis is the frequency of the perturbation signal as in bode plot; y-axis is the magnitude in DB or phase in degree, and z-axis is the running parameter, which is the switching frequency. This is because for resonant converter, to regulate the output voltage, the switching frequency will be varied. For different switching frequency, the small signal model will be different. From these results, following things can be clearly identified:

1. Beat frequency double pole. This is a special characteristic for resonant converter [5][6]. As switching frequency changes, a double pole with frequency at the difference of switching frequency and resonant frequency will move accordingly too. Finally, when switching frequency is close enough to resonant converter, this double pole will split, one merge with low frequency pole formed by output cap and load, one move to higher frequency.

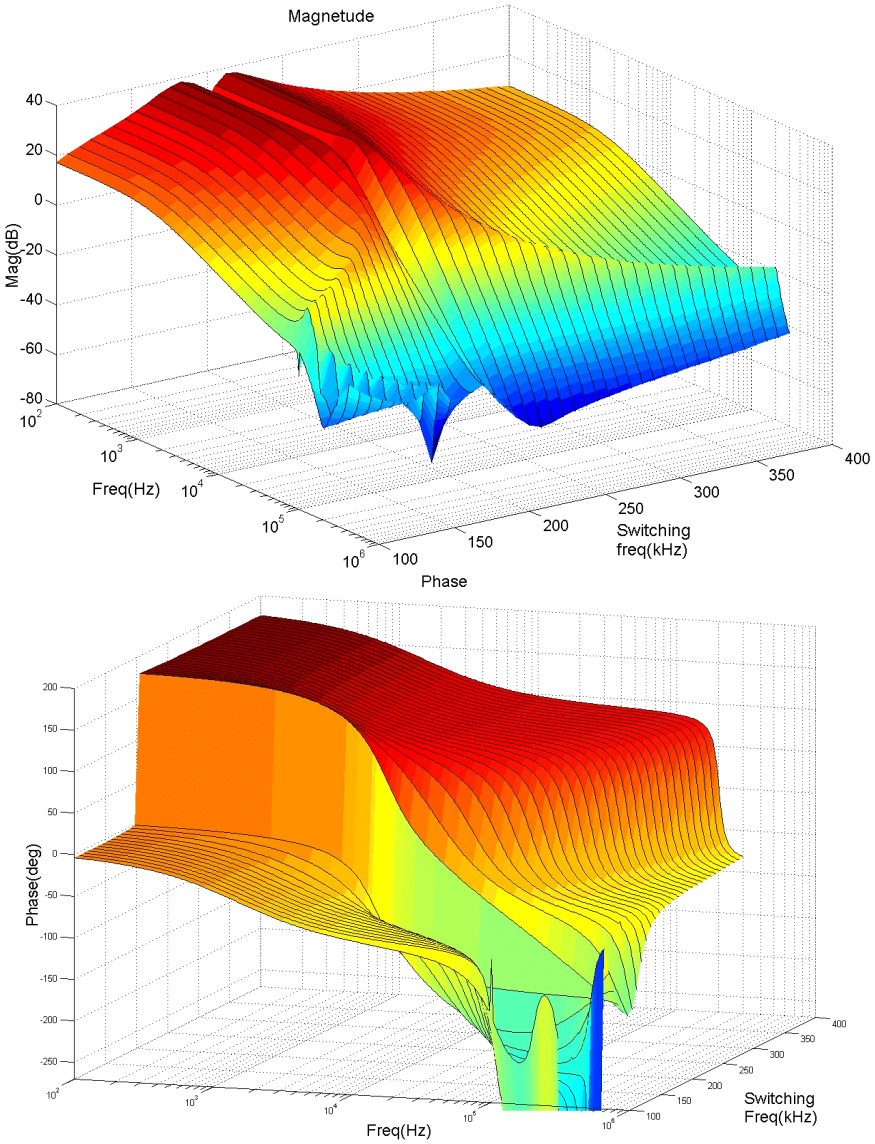

Figure C.2 Bode plot of control to output transfer function of Series Resonant Converter

2. Beat frequency dynamic. Since the low frequency gain is proportional to the slope of DC characteristic of series resonant converter. When the operation frequency moves close to the resonant frequency, the slope gets flat and low frequency gain drops. When switching frequency equals to resonant frequency, the gain will be zero. As can be clearly seen on the graph, when switching frequency is close to resonant frequency, the control to output gain will be very low. A gap can be observed on the graph.

3. The phase has a 180-degree jump around resonant frequency. This is because of the change of the DC characteristic slope. Switching frequency lower than resonant frequency, with increasing switching frequency, gain will increase, so the phase delay at DC will be zero. When the switching frequency is higher than resonant frequency, as switching frequency increases, gain will decrease, which will give 180 degree at DC.

4. Low frequency pole, which is caused by the output capacitor and load. With lighter load, this pole will move to lower frequency.

There should have an ESR zero if ESR of the output capacitor is considered. Here in this simulation, ESR is neglected.

From above simulation results, the small signal characteristic of a series resonant converter is derived. Beat frequency double pole and beat frequency dynamic are observed. Compare with results reported in [6], a very good match is achieved. From this result, we can be more confident with the method. These

results also will be used as a reference to compare with LLC resonant converter since it is very similar to SRC in some operating region.

Appendix D.

LLC converter model for EDF analysis

In this part, the model file and software package for extended describing function analysis will be listed. This software is written in MATLAB. This appendix is divided into two parts. First part is the process for building the model file for extended describing function analysis. In the second part, the LLC model file for extended describing function analysis at listed. The software package for extended describing function could be found in dissertation of Dr. Eric X. Yang. The version used for the analysis is MATLAB 5.0.

D.1. Process of building LLC circuit model for EDF analysis

To build the model of the converter for describing function analysis, first the operation of the converter need to be understood clearly. The operating stages in each switching cycle need to be identified. For each operating stage, the state space needs to be derived. Base on this information, the model file could be build.

In this part, the operating modes of LLC converter at full load condition will be analyzed in region 1 and region 2. Region 3 is eliminated because of ZCS operation. At light load condition, the converter might run into DCM. Since DCM

operation will introduce many more operating modes, it is not included in this model. The circuit and notifications are shown in Figure D.1.

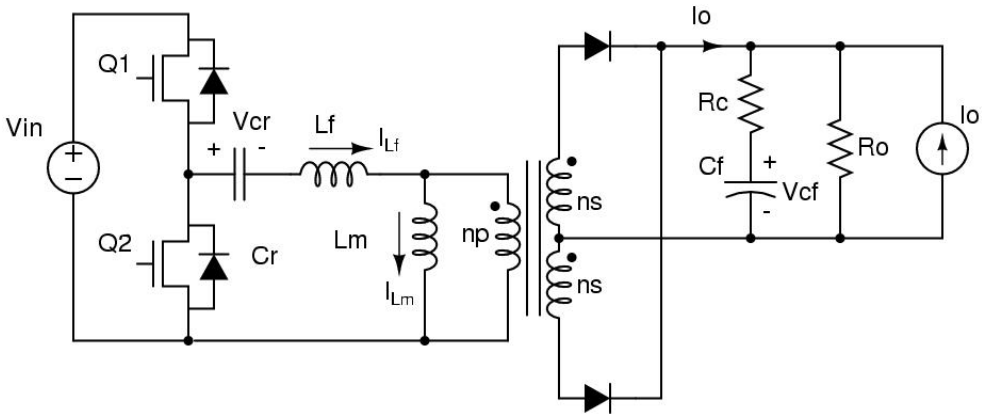

Figure D.1 Circuit diagram and notification for extended describing function analysis

In this circuit, there are four passive components: Lr, Cr, Lm and Co. Four states could be chosen for each components as: I_{Lr}, I_{Lm}, V_{Cr}, and V_{Co}. But look at the topology; the current through output is the difference of two states, I_{Lr} and I_{Lm}. Also, the converter changes stage if I_{Lr}-I_{Lm} changes sign as will shown later. For simplification, the states were chosen as: I_{Lr}-I_{Lm}, I_{Lm}, V_{Cr}, and V_{Co}. As shown in the circuit, the input variables are Vin and Io. The output variables are Iin and Vo. With these variables the state equations in each region could be derived in the form of:

$$\dot{x} = Ax + Bu$$
$$y = Cx + Du$$

$$x = \begin{pmatrix} i_{Lr} - i_{Lm} & i_{Lm} & v_{Cr} & v_{Cf} \end{pmatrix}'$$

where $u = \begin{pmatrix} v_{in} & i_o \end{pmatrix}'$.

$$y = \begin{pmatrix} v_o & i_{in} \end{pmatrix}'$$

D.1.1. Model of LLC resonant converter in region 1

The simulation waveforms of LLC resonant converter in region 1 are shown in Figure D.2. The operation in this region could be divided into 4 different modes as shown in the diagram. The simplified topology in each mode and the condition for transferring from one mode to next mode is shown in Figure D.3.

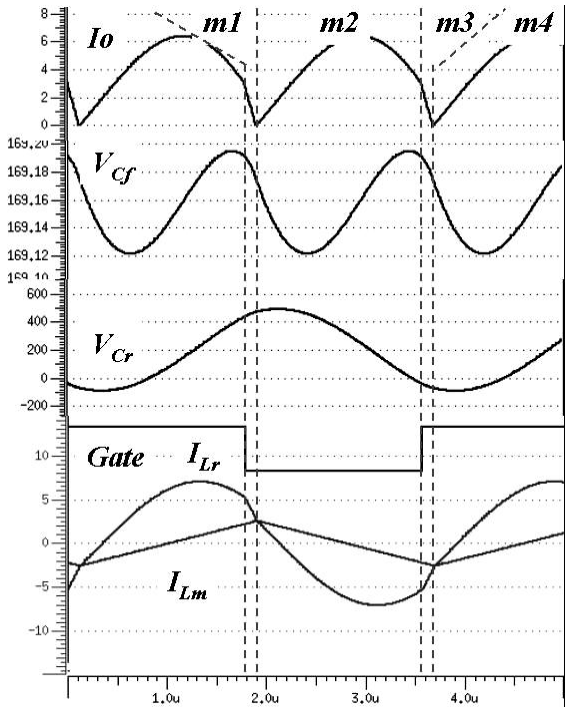

Figure D.2 Simulation waveform of LLC converter in region 1

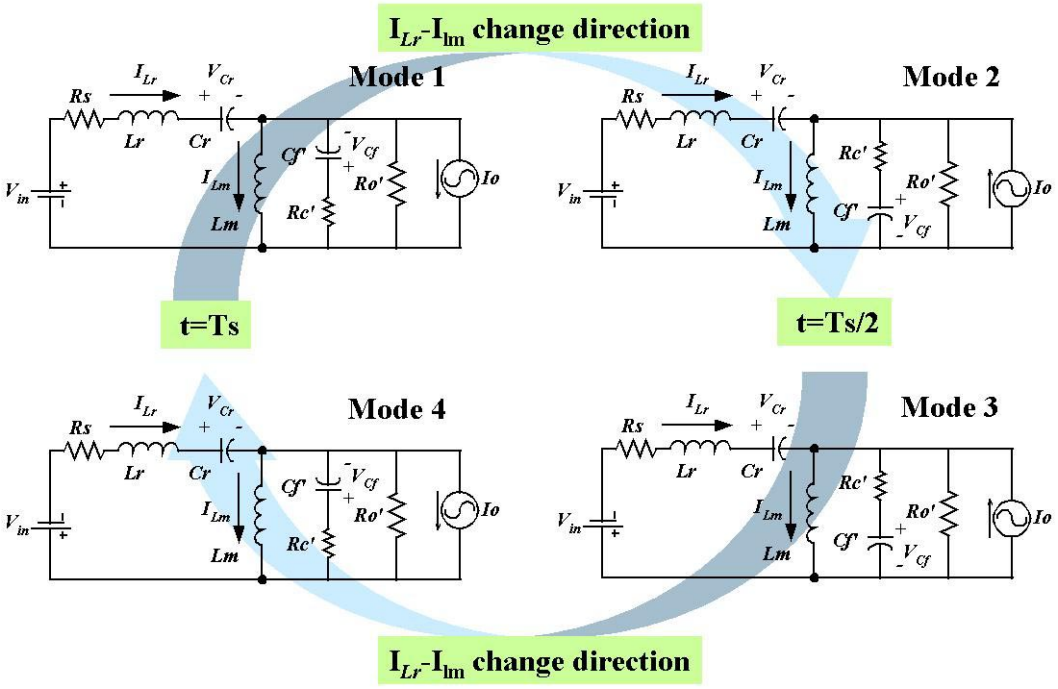

Figure D.3 Topology modes and progressing condition for region 1

The state equations for each mode are shown as following.

Mode 1

$$A=\begin{bmatrix} -\frac{Rs+R}{Lr} & -\frac{R}{Lm} & -\frac{Rs}{Lr} & -\frac{1}{Lr} & \frac{k}{Lr}+\frac{k}{Lm} \\ \frac{R}{Lm} & & 0 & 0 & -\frac{k}{Lm} \\ \frac{1}{Cr} & & \frac{1}{Cr} & 0 & 0 \\ -\frac{k}{Cf} & & 0 & 0 & -\frac{k}{R\cdot Cf} \end{bmatrix} \quad \text{Where} \quad R=Ro\,//\,Rc \quad k=\frac{R}{R+Rc}.$$

$$B=\begin{bmatrix} \frac{1}{Lr} & \frac{R}{Lr}+\frac{R}{Lm} \\ 0 & -\frac{R}{Lm} \\ 0 & 0 \\ 0 & \frac{k}{Cf} \end{bmatrix}$$

$$C=\begin{bmatrix} -R & 0 & 0 & k \\ 1 & 1 & 0 & 0 \end{bmatrix}$$

$$D=\begin{bmatrix} 0 & R \\ 0 & 0 \end{bmatrix}$$

Mode 2

$$A=\begin{bmatrix} -\frac{Rs+R}{Lr}-\frac{R}{Lm} & -\frac{Rs}{Lr} & -\frac{1}{Lr} & -\frac{k}{Lr}-\frac{k}{Lm} \\ \frac{R}{Lm} & 0 & 0 & \frac{k}{Lm} \\ \frac{1}{Cr} & \frac{1}{Cr} & 0 & 0 \\ \frac{k}{Cf} & 0 & 0 & -\frac{k}{R\cdot Cf} \end{bmatrix}$$

$$B=\begin{bmatrix} \frac{1}{Lr} & -\frac{R}{Lr}-\frac{R}{Lm} \\ 0 & \frac{R}{Lm} \\ 0 & 0 \\ 0 & \frac{k}{Cf} \end{bmatrix}$$

$$C=\begin{bmatrix} R & 0 & 0 & k \\ 1 & 1 & 0 & 0 \end{bmatrix}$$

$$D = \begin{bmatrix} 0 & R \\ 0 & 0 \end{bmatrix}$$

Mode 3

$$A = \begin{bmatrix} -\frac{Rs+R}{Lr} & -\frac{R}{Lm} & -\frac{Rs}{Lr} & -\frac{1}{Lr} & -\frac{k}{Lr} - \frac{k}{Lm} \\ \frac{R}{Lm} & & 0 & 0 & \frac{k}{Lm} \\ \frac{1}{Cr} & & \frac{1}{Cr} & 0 & 0 \\ \frac{k}{Cf} & & 0 & 0 & -\frac{k}{R \cdot Cf} \end{bmatrix}$$

$$B = \begin{bmatrix} -\frac{1}{Lr} & -\frac{R}{Lr} - \frac{R}{Lm} \\ 0 & \frac{R}{Lm} \\ 0 & 0 \\ 0 & \frac{k}{Cf} \end{bmatrix}$$

$$C = \begin{bmatrix} R & 0 & 0 & k \\ -1 & -1 & 0 & 0 \end{bmatrix}$$

$$D = \begin{bmatrix} 0 & R \\ 0 & 0 \end{bmatrix}$$

Mode 4

$$A=\begin{bmatrix} -\frac{Rs+R}{Lr} & -\frac{R}{Lm} & -\frac{Rs}{Lr} & -\frac{1}{Lr} & \frac{k}{Lr}+\frac{k}{Lm} \\ \frac{R}{Lm} & & 0 & 0 & -\frac{k}{Lm} \\ \frac{1}{Cr} & & \frac{1}{Cr} & 0 & 0 \\ -\frac{k}{Cf} & & 0 & 0 & -\frac{k}{R\cdot Cf} \end{bmatrix}$$

$$B=\begin{bmatrix} -\frac{1}{Lr} & \frac{R}{Lr}+\frac{R}{Lm} \\ 0 & -\frac{R}{Lm} \\ 0 & 0 \\ 0 & \frac{k}{Cf} \end{bmatrix}$$

$$C=\begin{bmatrix} -R & 0 & 0 & k \\ -1 & -1 & 0 & 0 \end{bmatrix}$$

$$D=\begin{bmatrix} 0 & R \\ 0 & 0 \end{bmatrix}$$

D.1.2. Model of LLC resonant converter in region 2

The simulation waveforms of LLC resonant converter in region 2 are shown in Figure D.4. The operation in this region also could be divided into 4 different modes as shown in the diagram. The simplified topology in each mode and the condition for transferring from one mode to next mode is shown in Figure D.5.

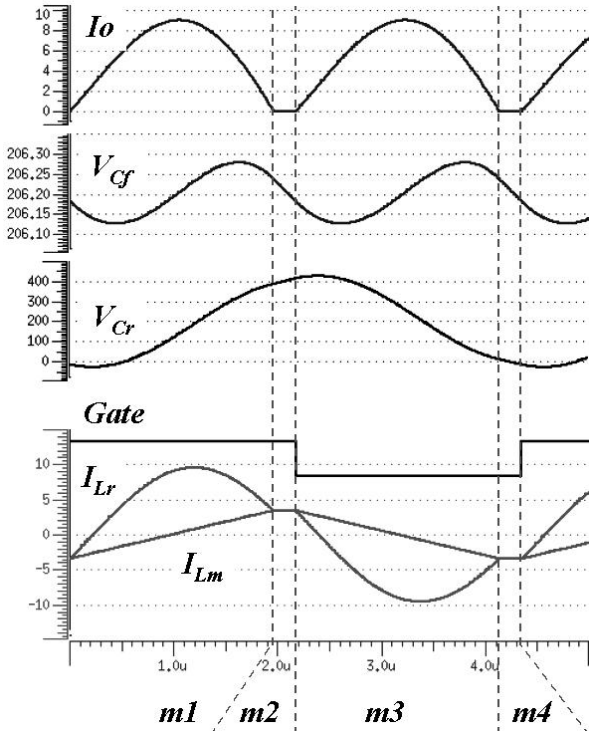

Figure D.4 Simulation waveform of LLC converter in region 2

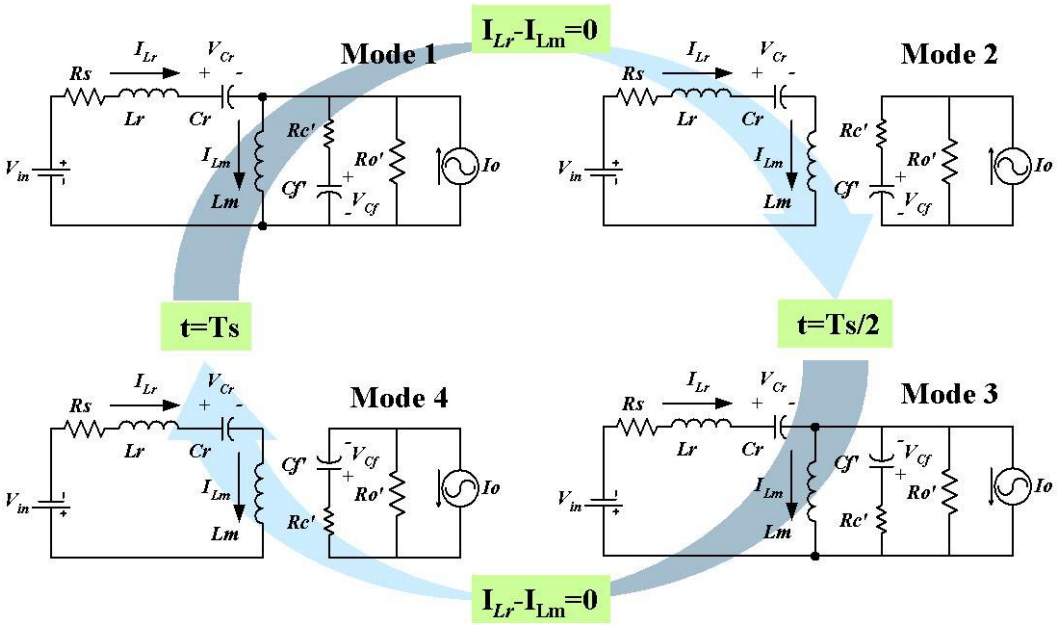

Figure D.5 Topology modes and progressing condition for region 2

The state equations for each mode are shown as following.

Mode 1

$$A=\begin{bmatrix} -\frac{Rs+R}{Lr} & -\frac{R}{Lm} & -\frac{Rs}{Lr} & -\frac{1}{Lr} & -\frac{k}{Lr}-\frac{k}{Lm} \\ \frac{R}{Lm} & & 0 & 0 & \frac{k}{Lm} \\ \frac{1}{Cr} & & \frac{1}{Cr} & 0 & 0 \\ \frac{k}{Cf} & & 0 & 0 & -\frac{k}{R\cdot Cf} \end{bmatrix}$$

$$B=\begin{bmatrix} \frac{1}{Lr} & -\frac{R}{Lr}-\frac{R}{Lm} \\ 0 & \frac{R}{Lm} \\ 0 & 0 \\ 0 & \frac{k}{Cf} \end{bmatrix}$$

$$C=\begin{bmatrix} R & 0 & 0 & k \\ 1 & 1 & 0 & 0 \end{bmatrix}$$

$$D=\begin{bmatrix} 0 & R \\ 0 & 0 \end{bmatrix}$$

Mode 2

$$A=\begin{bmatrix} 0 & 0 & 0 & 0 \\ 0 & -\dfrac{Rs}{Lm+Lr} & -\dfrac{1}{Lm+Lr} & 0 \\ 0 & \dfrac{1}{Cr} & 0 & 0 \\ 0 & 0 & 0 & -\dfrac{k}{R\cdot Cf} \end{bmatrix}$$

$$B=\begin{bmatrix} 0 & 0 \\ \dfrac{1}{Lr+Lm} & 0 \\ 0 & 0 \\ 0 & \dfrac{k}{Cf} \end{bmatrix}$$

$$C=\begin{bmatrix} 0 & 0 & 0 & k \\ 1 & 1 & 0 & 0 \end{bmatrix}$$

$$D=\begin{bmatrix} 0 & R \\ 0 & 0 \end{bmatrix}$$

Mode 3

$$A=\begin{bmatrix} -\dfrac{Rs+R}{Lr} & -\dfrac{R}{Lm} & -\dfrac{Rs}{Lr} & -\dfrac{1}{Lr} & \dfrac{k}{Lr}+\dfrac{k}{Lm} \\ \dfrac{R}{Lm} & & 0 & 0 & -\dfrac{k}{Lm} \\ \dfrac{1}{Cr} & & \dfrac{1}{Cr} & 0 & 0 \\ -\dfrac{k}{Cf} & & 0 & 0 & -\dfrac{k}{R\cdot Cf} \end{bmatrix}$$

$$B=\begin{bmatrix} -\frac{1}{Lr} & \frac{R}{Lr}+\frac{R}{Lm} \\ 0 & -\frac{R}{Lm} \\ 0 & 0 \\ 0 & \frac{k}{Cf} \end{bmatrix}$$

$$C=\begin{bmatrix} -R & 0 & 0 & k \\ -1 & -1 & 0 & 0 \end{bmatrix}$$

$$D=\begin{bmatrix} 0 & R \\ 0 & 0 \end{bmatrix}$$

Mode 4

$$A=\begin{bmatrix} 0 & 0 & 0 & 0 \\ 0 & -\frac{Rs}{Lm+Lr} & -\frac{1}{Lm+Lr} & 0 \\ 0 & \frac{1}{Cr} & 0 & 0 \\ 0 & 0 & 0 & -\frac{k}{R\cdot Cf} \end{bmatrix}$$

$$B=\begin{bmatrix} 0 & 0 \\ -\frac{1}{Lr+Lm} & 0 \\ 0 & 0 \\ 0 & \frac{k}{Cf} \end{bmatrix}$$

$$C=\begin{bmatrix} 0 & 0 & 0 & k \\ -1 & -1 & 0 & 0 \end{bmatrix}$$

$$D = \begin{bmatrix} 0 & R \\ 0 & 0 \end{bmatrix}$$

With above information, the model file could be written as shown next.

D.2. LLC resonant converter model

Following is the model file for LLC resonant converter. It covers the operating region 1 and 2. Region 3 is now covered since it is ZCS and not preferred for this converter. This model file only deals with the normal operation mode. During very light load condition, the converter might work into different discontinuous conduction modes. To cover these operation modes, the model file needs to be extended. The method of building the model file is demonstrated in chapter 4.

```
%%%%%%%%%%%%%%%%%%%%%%%%%%%%%%%%%%%%%%%%%%%%%%%%%%%%%%%%%%%
% Name:    topo.m --------  LLC topology for continuous condition mode
% Build by:  Bo Yang, Dec. 2001
% Function:  define converter circuit, operating condition,
%          and switching boundary condition
% Input:     CP ------------  Circuit Parameters
%          x ------------- current state vector
%          u ------------- current input vector
%          contl ---------  control parameters
%          cur_mode ------ current topological mode
%          t ------------- current time
%
% Output:    num_mode ------  # of modes in one cycle
%          Para ----------  Circuit Parameters
%          x0 ------------ initial condition
%          U0 ------------ given input vector
%          CTL -----------  Control Parameters
%          harm_tbl ------ harmonic table (see Chap.3)
%          switching -----  1 = not cross switching boundary
%                     -1 = cross switching boundary
%          A, B, C, D ---- state matrices of current mode
%          Ab,Bb,Cb,Db---- boundary matrices of current mode
%
% Calling:   none
%
%%%%%%%%%%%%%%%%%%%%%%%%%%%%%%%%%%%%%%%%%%%%%%%%%%%%%%%%%%%

function [RT1, RT2, RT3, RT4, RT5, RT6, Bb, Cb, Db, Fo, Zo] ...
    = topo(CP, x, u, contl, cur_mode, t)
```

```
%%%%%%%%%%%%%%%%%%%  State Equation Description  %%%%%%%%%%%%%%%%%%
% Input:     U = [Vg, Io];
% Output:    Y = [Vo, Ig];
% State:     X = [Ilr, Ilm, Vcr, Vcf];
%%%%%%%%%%%%%%%%%%%%%%%%%%%%%%%%%%%%%%%%%%%%%%%%%%%%%%%%%%%%%%%%

% define # of mode and dimension of output
num_mode = 4;

% define harmonic table
%           dc  1st  2nd  3rd  4th  5th
harm_tbl = [0    1    0    1    0    1   0   1;          % Ilr-Ilm -- 1st state
            0    1    0    1    0    1   0   1;             % Ilm -- 2nd state
            0    1    0    1    0    1   0   1;           % Vcr -- 3nd state
            1    0    0    0    0    0   0   0];             % vo - 4rd state

% define circuit parameters: [Lr; Cr; Lm; Cf; rs; rc; Qs]
Para = [22.5e-6; 28e-9; 60e-6; 20e-6; 0.01; 0.01; 0.5];

% define initial condition
x0 = [0;  -5;  -300; 190];                  % [Ilr-Ilm; Ilm; Vcr; vcf]

% define Input variables
U0 = [200; 0];                              % [Vg, Io]

% define control variables
CTL = [0.99*200e3];                         % Fs; Frequency control

if nargin == 0,
    RT1 = num_mode;
    RT2 = Para;
    RT3 = x0;
    RT4 = U0;
    RT5 = CTL;
    RT6 = harm_tbl;
    return;

elseif nargin == 6,
    Lr = CP(1);
    Cr = CP(2);
    Lm = CP(3);
    Cf = CP(4);
    rs = CP(5);
    rc = CP(6);
    Qs = CP(7);                             % Qs=Zo/R;

    Fs = contl(1);

    % Some parameters
    Zo = sqrt(Lr/Cr);                       % Zo
    Fo = 1/(2*pi*sqrt(Lr*Cr));                  % Fo=200 kHz;
    R = Zo / Qs;

    % Fsn = Fs / Fo;

    k  = R / (R+rc);
    r = k * rc;
    Ts = 1/Fs;

    % define switching boundary conditions

    if cur_mode == 1,

        Si=1;                               % rectifier polarity
        St=1;                               % active bridge polarity

        % set crossing boundary flag
```

```
    if x(1) < 0.0 ,
        switching = -1;
    else
        switching = 1;
    end

    % define piecewise linear state equations
    A = [(-rs-r)/Lr,    -rs/Lr,     -1/Lr,      -k/Lr;
        r/Lm,           0,          0,          k/Lm;
        1/Cr,           1/Cr,       0,          0;
        k/Cf,           0,          0,          -k/R/Cf];
    B = [1/Lr,          -r/Lr;
        0,              r/Lm;
        0,              0;
        0,            k/Cf];
    C = [r,             0,          0,          k;
        1,              1,          0,          0];
    D = [0,   r;
        0,   0];

    % switching boundary condition:
    % Ab * x + Bb * u + Cb * t + Db < 0
    Ab = [1, 0, 0, 0];

    Bb = [0, 0];
    Cb = 0;
    Db = 0;

elseif cur_mode == 2,

    Si=-1;
    St=1;

    if t > 0.5 * Ts;
        switching = -1;
    else
        switching = 1;
    end

    % define piecewise linear state equations
    A = [0,             0,          0,          0;
        0,              -rs/(Lm+Lr) -1/(Lm+Lr), 0;
        0,           1/Cr,       0,          0;
        0,              0,          0,          -k/R/Cf];
    B = [0,             0;
        1/(Lm+Lr)       0;
        0,              0;
        0,              k/Cf];
    C = [0,             0,          0,          k;
        1,              1,          0,          0];
    D = [0,   r;
        0,   0];

    Ab = [0, 0, 0, 0];
    Bb = [0, 0];
    Cb = 0;
    Db = 0;

elseif cur_mode == 3,

    Si=-1;
    St=-1;

    if x(1) > 0,
        switching = -1;
    else,
        switching = 1;
```

```
        end,

        % define piecewise linear state equations
        A = [(-rs-r)/Lr,    -rs/Lr,     -1/Lr,      k/Lr;
            r/Lm,           0,          0,          -k/Lm;
            1/Cr,           1/Cr,       0,          0;
            -k/Cf,           0,          0,          -k/R/Cf];
        B = [-1/Lr,          r/Lr;
            0,              -r/Lm;
            0,              0;
            0,            k/Cf];
        C = [-r,             0,          0,          k;
            -1,              -1,          0,          0];
        D = [0,   r;
            0,   0];

        Ab = [-1, 0, 0, 0];
        Bb = [0, 0];
        Cb = 0;
        Db = 0;

    elseif cur_mode == 4,

        Si=1;
        St=-1;

        if t > Ts,
            switching = -1;
        else
            switching = 1;
        end

        % define piecewise linear state equations
        A = [0,             0,          0,          0;
            0,              -rs/(Lm+Lr) -1/(Lm+Lr), 0;
            00,           1/Cr,       0,          0;
            0,              0,          0,          -k/R/Cf];
        B = [0,             0;
            -1/(Lm+Lr),     0;
            0,              0;
            0,              k/Cf];
        C = [0,             0,          0,          k;
            -1,             -1,         0,          0];
        D = [0,   r;
            0,   0];

        Ab = [0, 0, 0, 0];
        Bb = [0, 0];
        Cb = 0;
        Db = 0;

    end


    RT1 = switching;
    RT2 = A;
    RT3 = B;
    RT4 = C;
    RT5 = D;
    RT6 = Ab;

    return;

else,
    error('ERROR USE OF TOPO()!!');
end
```

Reference

A. Distributed power system and PWM topologies

[A-1] IBM Corporation, *1999 IBM Power Technology Symposium, Theme: DC/DC Conversion*, September 1999, Research Triangle Park, NC.

[A-2] Intel Corporation, *Intel Power Supply Technology Symposium*, June 1998, Dupont, WA.

[A-3] Intel Corporation, *Intel Power Supply Technology Symposium*, September 2000.

[A-4] C.C. Heath, "The Market For Distributed Power Systems," *Proc. IEEE APEC '91,* 1991, 10-15 March 1991 pp. 225 –229.

[A-5] W.A. Tabisz, M.M. Jovanovic, and F.C. Lee, "Present And Future Of Distributed Power Systems," *Proc. IEEE APEC '92*, 1992, pp. 11 –18.

[A-6] F.C. Lee, P. Barbosa, P. Xu; J. Zhang; B. Yang; Canales, F., "Topologies And Design Considerations For Distributed Power System Applications," *Proceedings of the IEEE, Volume: 89 Issue: 6*, June 2001 Page(s): 939 – 950.

[A-7] Mazumder, Sudip K. Shenai, Krishna, "On The Reliability Of Distributed Power Systems: A Macro- To Micro- Level Overview Using A Parallel Dc-Dc Converter," *Proc. IEEE PESC,* 2002, pp. 809-814.

[A-8] Hua, G.C., Tabisz, W.A., Leu, C.S., Dai, N., Watson, R., Lee, F.C., "Development Of A DC Distributed Power System," *Proc. IEEE APEC '94.* 1994,pp. 763 -769 vol.2.

[A-9] G.S. Leu, G. Hua, and F.C. Lee, "Comparison of Forward Circuit Topologies with various reset scheme," *VPEC 9th Seminar,* 1991.

[A-10] Min Chen, Dehong Xu, M. Matsui, "Study On Magnetizing Inductance Of High Frequency Transformer In The Two Transistor Forward Converter," *Proc. Power Conversion Conference,* 2002, pp. 597-602.

[A-11] Jianping Xu, Xiaohong Cao, Qianchao Luo, "An Improved Two Transistor Forward Converter," *Proc. IEEE PEDS,* 1999, pp. 225-228.

[A-12] W. Chen, F.C. Lee, M.M. Jovanovic, J.A. Sabate, "A Comparative Study Of A Class Of Full Bridge Zero Voltage Switched PWM Converters," *Proc. IEEE APEC,* 1995, pp. 893-899.

[A-13] A.W. Lotfi, Q. Chen, F.C. Lee, "A Nonlinear Optimization Tool For The Full Bridge Zero Voltage Switched DC-DC Converter," *Proc. IEEE PESC '92,* 1992, pp. 1301-1309.

[A-14] Xinbo Ruan; Yangguang Yan, "Soft-Switching Techniques For PWM Full Bridge Converters," *Proc. IEEE PESC '00,* 2000, pp. 634 -639 vol.2.

[A-15] D.B. Dalal, F.S. Tsai, "A 48V, 1.5kw, Front-End Zero Voltage Switches PWM Converter With Lossless Active Snubbers For Output Rectifiers," *Proc. IEEE APEC 93,* 1993, pp. 722-728.

[A-16] J.G. Cho, J.A. Sabate, G. Hua, and F.C. Lee, "Zero Voltage And Zero Current Switching Full Bridge PWM Converter For High Power Applications," *Proc. IEEE PESC '94*, 1994.

[A-17] J.H. Liang, Po-chueh Wang, Kuo-chien Huang, Cern-Lin Chen, Yi-Hsin Leu, Tsuo-Min chen, " Design Optimization For Asymmetrical Half Bridge Converters," *Proc. IEEE APEC '01,* 2001, pp. 697-702, vol.2.

[A-18] Y. Leu, C. Chen, "Analysis and Design of Two-Transformer Asymmetrical Half-Bridge Converter," *Proc. IEEE PESC '02*, 2002, pp. 943-948.

[A-19] S. Korotkov, V. Meleshin, R. Miftahutdinov, S. Fraidlin, "Soft Switched Asymmetrical Half Bridge DC/DC Converter: Steady State Analysis. An Analysis of Switching Process," *Proc. Telescon '97*,. 1997, pp. 177-184.

[A-20] L. Krupskiy, V. Meleshine, A. Nemchinov, "Unified Model of the Asymmetrical Half Bridge for Three Important Topological Variations," *Proc. IEEE INTELEC '99,* 1999, pp.8.

[A-21] L. Krupskiy, V. Meleshine, A. Nemchinov, "Small Signal Modeling of Soft Switched Asymmetrical Half Bridge DC/DC Converter," *Proc. IEEE APEC '95,* 1995, pp. 707-711.

[A-22] W. Chen, P. Xu, F.C. Lee, "The Optimization Of Asymmetrical Half Bridge Converter," *Proc. IEEE APEC '01,* 2001, pp. 603-707, vol.2.

[A-23] P. Wong, B. Yang, P. Xu and F.C. Lee, "Quasi Square Wave Rectifier For Front End DC/DC Converters," *Proc. IEEE PESC '00,* 2000, pp. 1053-1057, vol.2.

[A-24] B. Yang, P. Xu, and F.C. Lee, "Range Winding For Wide Input Range Front End DC/DC Converter," *Proc. IEEE APEC,* 2001, pp. 476-479.

[A-25] G. Hua, and F.C. Lee, "An Overview of Soft-Switching Techniques for PWM Converters," *Proc. IPEMC '94,* 1994.

B. Resonant converter

[B-1] R. Oruganti and F.C. Lee, "Resonant Power Processors, Part 2: Methods of Control," *IEEE Trans. on Industrial Application*, 1985.

[B-2] R. Severns, "Topologies For Three Element Resonant Converters," Proc. IEEE APEC '90, 1990, pp. 712-722.

[B-3] Vatche Vorperian, Analysis Of Resonant Converters, Dissertation, California Institute of Technology, 1984.

[B-4] R. Farrington, M.M. Jovanovic, and F.C. Lee, "Analysis of Reactive Power in Resonant Converters," Proc. IEEE PESC '92, 1992.

[B-5] P. Calderira, R. Liu, D. Dalal, W.J. Gu, "Comparison of EMI Performance of PWM and Resonant Power Converters," Proc. IEEE PESC '93, 1993, pp. 134-140.

[B-6] T. Higashi, H. Tsuruta, M. Nakahara, "Comparison of Noise Characteristics for Resonant and PWM Flyback Converters," Proc. IEEE PESC '98, 1998, pp. 689-695.

[B-7] K.H. Liu, "Resonant Switches Topologies and Characteristics," Proc. IEEE PESC'85, 1985, pp. 106-116.

[B-8] R. Oruganti and F.C. Lee, "Effect of Parasitic Losses on the Performance of Series Resonant Converters," *Proc. IEEE IAS, '85,* 1985.

[B-9] R. Oruganti, J. Yang, and F.C. Lee, "Implementation of Optimal Trajectory Control of Series Resonant Converters," *Proc. IEEE PESC '87,* 1987.

[B-10] A.K.S. Bhat, "Analysis and Design of a Modified Series Resonant Converter," *IEEE Trans. on Power Electronics*, 1993, pp. 423-430.

[B-11] J.T. Yang and F.C. Lee, "Computer Aided Design and Analysis of Series Resonant Converters," *Proc. IEEE IAS '87,* 1987.

[B-12] V. Vorperian and S. Cuk, "A Complete DC Analysis of the Series Resonant Converter," Proc. IEEE PESC'82, 1982.

[B-13] F.S. Tsai, and F.C. Lee, "A Complete DC Characterization of a Constant-Frequency, Clamped-Mode, Series Resonant Converter," Proc IEEE PESC'88, 1988.

[B-14] R. Oruganti, J. Yang, and F.C. Lee, "State Plane Analysis of Parallel Resonant Converters," Proc. IEEE PESC '85, 1985.

[B-15] R. Liu, I. Batarseh, C.Q. Lee, "Comparison of Capacitively and Inductively Coupled Parallel Resonant Converters," IEEE Trans. on Power Electronics, 1993, pp. 445-454, vol.8, issue 4.

[B-16] M. Emsermann, "An Approximate Steady State and Small Signal Analysis of the Parallel Resonant Converter Running Above Resonance," *Proc. Power* Electronics *and Variable Speed Drives '91*, 1991, pp. 9-14.

[B-17] Y.G. Kang, A.K. Upadhyay, D. Stephens, "Analysis and Design of a Half Bridge Parallel Resonant Converter Operating Above Resonance," *Proc. IEEE IAS '98,* 1998, pp. 827-836.

[B-18] Robert L. Steigerwald, "A Comparison of Half Bridge Resonant Converter Topologies," *IEEE Trans. on Power Electronics*, 1988, pp. 174-182.

[B-19] M. Zaki, A. Bonsall, I. Batarseh, "Performance Characteristics for the Series Parallel Resonant Converter," *Proc. Southcon '94*, 1994, pp.573-577.

[B-20] A.K.S. Bhat, "Analysis, Optimization and Design of a Series Parallel Resonant Converter," *Proc. IEEE APEC '90*, 1990, pp. 155-164.

[B-21] H. Jiang, G. Maggetto, P. Lataire, "Steady State Analysis of the Series Resonant DC/DC Converter in Conjunction with Loosely Coupled Transformer Above Resonance Operation," IEEE Trans. on Power Electronics, 1999, pp. 469-480.

[B-22] R. Liu, C.Q. Lee, and A.K. Upadhyay, "A Multi Output LLC-Type Parallel Resonant Converter," IEEE Trans. on Aerospace and Electronic Systems, 1992, pp. 697-707, vol.28, issue 3.

[B-23] A.K.S. Bhat, "Analysis and Design of a Series Parallel Resonant Converter With Capacitive Output Filter," Proc. IEEE IAS '90, 1990, pp. 1308-1314.

[B-24] R. Liu, and C.Q. Lee, "Series Resonant Converter with Third-Order Commutation Network," *IEEE Trans. on Power Electronics*, 1992, pp. 462-467, vol.7, issue 3.

[B-25] J.F. Lazar, R. Martinelli, "Steady State Analysis of the LLC Series Resonant Converter," Proc. IEEE APEC'01, 2001, pp.728-735.

[B-26] R. Elferich, T. Duerbaum, "A New Load Resonant Dual Output Converter," Proc. IEEE PESC'02, 2002, pp.1319-1324.

[B-27] B. Yang, F.C. Lee, A.J. Zhang and G. Huang, "LLC Resonant Converter For Front End DC/DC Conversion," *Proc. IEEE APEC,* 2002, pp. 1108-1112 vol.2.

C. Integrated Magnetic

[C-1] P. -L. Wong, P. Xu, B. Yang and F. C. Lee, "Performance Improvements of Interleaving VRMs with Coupling Inductors," *Proc. CPES Annual Seminar*, 2000, pp. 317-324.

[C-2] B. Mohandes, "Integrated PC Board Transformers Improve High Frequency PWM Converter Performance," *PCIM Magazine*, July 1994.

[C-3] I. Jitaru and A. Ivascu, "Increasing the Utilization of the Transformer's Magnetic Core by Using Quasi-Integrated Magnetics," *Proc. HFPC Conf.*, 1996, pp. 238-252.

[C-4] C. Peng, M. Hannigan, O. Seiersen, "A New Efficient High Frequency Rectifier Circuit", *Proc. HFPC Conf.,* 1991, pp. 236-243.

[C-5] P. Xu, Q. Wu, P.-L. Wong and F. C. Lee, "A Novel Integrated Current Doubler Rectifier," *Proc. IEEE APEC*, 2000, pp. 735-740.

[C-6] S. Cuk, "New Magnetic Structures for Switching Converters," *IEEE Transaction On Magnetics*, March 1983, pp. 75-83.

[C-7] S. Cuk, L. Stevanovic and E. Santi, "Integrated Magnetic Design with Flat Low Profile Core," *Proc. HFPC Conf.*, 1990.

[C-8] I. W. Hofsajer, J. D. van Wyk and J. A. Ferreira, "Volume Considerations of Planar Integrated Components," *Proc. IEEE PESC*, 1999, pp. 741-745.

[C-9] D. Y. Chen, "Comparison of High Frequency Magnetic Core Loss under Two Different Driving Conditions: A Sinusoidal Voltage and a Square-Wave," *Proc. IEEE PESC*, 1978, pp. 237-241.

[C-10] N. Dai and F. C. Lee, "Edge Effect Analysis in a High-Frequency Transformer," *Proc. IEEE PESC*, 1994, pp. 850-855.

[C-11] W. M. Chew and P. D. Evans, "High Frequency Inductor Design Concept," *Proc. IEEE PESC*, 1991, pp. 673-678.

[C-12] K. D. T. Ngo and M. H. Kuo, "Effects of Air Gaps on Winding Loss in High-Frequency Planar Magnetics," *Proc. IEEE PESC*, 1988, pp. 1112-1119.

[C-13] L. Ye, R. Wolf and F. C. Lee, "Some Issues of Loss Measurement and Modeling for Planar Inductors," *Philips Fellowship Report*, VPEC, September 1997.

[C-14] N. Dai, *Modeling, Analysis, and Design of High-Frequency, High-Density, Low-Profile Transformers*, Dissertation, Virginia Tech, Blacksburg, VA, 1996.

[C-15] M. T. Zhang, M. M. Jovanovic and F. C. Lee, "Analysis, Design and Evaluation of Forward Converter with Distributed Magnetics – Interleaving and Transformer Paralleling," *Proc. IEEE APEC*, 1995, pp. 315-321.

[C-16] R. Prieto, J. A. Cobos, O. Garcia and J. Uceda. "Interleaving Techniques in Magnetic Components," *Proc. IEEE APEC*, 1997, pp. 931-936.

[C-17] Rengang Chen; Canales, F.; Bo Yang; van Wyk, J.D., "Volumetric Optimal Design Of Passive Integrated Power Electronic Module (IPEM) For Distributed Power System (DPS) Front-End DC/DC Converter," *Proc. IEEE IAS*, 13-18 Oct. 2002 pp. 1758 -1765 vol.3.

[C-18] Rengang Chen, J.T. Strydom, J.D. Van Wyk, "Design Of Planar Integrated Passive Module For Zero Voltage Switched Asymmetrical Half Bridge PWM Converter," *Proc. IEEE IAS,* 2001, pp. 2232-2237 vol.4.

[C-19] B. Yang, Rengang Chen, and F.C. Lee, "Integrated Magnetic For LLC Resonant Converter," *Proc. IEEE APEC,* 2002, pp. 346-351, vol.1.

[C-20] Chen, Rengang. Yang, Bo. Canales, F. Barbosa, P. Van Wyk, J D. Lee, F C. "Integration Of Electromagnetic Passive Components In DPS Front-

End DC/DC Converter - A Comparative Study Of Different Integration Steps," *Proc. IEEE APEC*. 2003. p 1137-1142.

[C-21] P. -L. Wong, Q. Wu, P. Xu, B. Yang and F. C. Lee, "Investigating Coupling Inductor in Interleaving QSW VRM," *Proc. IEEE APEC Conf.,* 2000, pp. 973-978.

[C-22] W. –J Gu, R. Liu, "A Study of Volume and Weight vs. Frequency for High-Frequency Transformers," *Proc. IEEE PESC '93*, 1993, pp. 1123-1129.

[C-23] H.A. Kojori, J.D. Lavers, S.B. Dewan, "State Plane Analysis of a Resonant DC-DC Converter Incorporating Integrated Magnetic," *IEEE Trans. on Magnetics*, 1988, pp. 2898-2900.

[C-24] A. Kats, G. Ivensky, S. Ben-Yaakov, "Application of Integrated Mangetics in Resonant Converters," *Proc. IEEE APEC'97*, 1997, pp. 925-930.

D. Small Signal Modeling

[B-1] G. W. Wester and R. D. Middlebrook, "Low-Frequency Characterization of Switched DC-to-DC Converters," *Proc. IEEE PESC*, 1972, pp. 9-20.

[B-2] R. D. Middlebrook, "Measurement of Loop Gain in Feedback Systems," *Int. J. Electronics*, 1975, pp. 485-512.

[B-3] R. D. Middlebrook and S. Cuk, "A General Unified Approach to Modeling Switching-Converter Power Stages," *Proc. IEEE PESC*, 1976.

[B-4] R. Tymerski and V. Vorperian, "Generation, Classification and Analysis of Switched-Mode DC-to-DC Converters by the Use of Converter Cells," *Proc. INTELEC*, 1986, pp. 181-195.

[B-5] V. Vorperian, "Simplified Analysis of PWM Converters Using Model of PWM Switch, Part I: Continuous Conduction Mode," *IEEE Trans. on Aerospace and Electronic Systems*, 1990, pp. 490-496.

[B-6] V. Vorperian, "High Q Approximate Small Signal Analysis of Resonant Converters," *VPEC Seminar 1984*.

[B-7] V. Vorperian, "Simplified Analysis of PWM Converters Using Model of PWM Switch, Part II: Discontinuous Conduction Mode," *IEEE Trans. on Aerospace and Electronic Systems*, 1990, pp. 497-505.

[B-8] J. O. Groves and F. C. Lee, "Small Signal Analysis of Systems with Periodic Operating Trajectories," *Proc. VPEC Annual Seminar*, 1988, pp. 224-235.

[B-9] J. O. Groves, "Small-Signal Analysis Using Harmonic Balance Methods," *Proc. IEEE PESC*, 1991, pp. 74–79.

[B-10] E. X. Yang, "Extended Describing Function Method for Small-Signal Modeling of Switching Power Circuit," *Proc. VPEC Annual Seminar*, 1994, pp.87-96.

[B-11] E. X. Yang, F. C. Lee and M. Jovanovic, "Small-Signal Modeling of Series and Parallel Resonant Converters," *Proc. IEEE APEC*, 1992, pp. 785-792.

[B-12] Eric X. Yang, *Extended Describing Function Method for Small-Signal Modeling of Resonant and Multi-Resonant Converters*, Dissertation, Virginia Tech, Blacksburg, VA, February 1994.

[B-13] R.C. Wong and J. O. Groves, "An Automated Small-Signal Frequency-Domain Analyzer for General Periodic-Operating Systems as Obtained via Time-Domain Simulation," *Proc. IEEE PESC*, 1995, pp. 801-808.

E. General Textbooks

[E-1] N. Mohan, T. Undeland and W. Robbins, *Power Electronics*, 1995.

[E-2] Abraham I. Pressman, *Switching Power Supply Design,* 1991.

[E-3] Rudolf P. Severns, *Modern DC-To-DC Switchmode Power Converter Circuits,* 1985.

[E-4] J.K. Watson, *Applications Of Magnetism,* 1985

Vita

The author, Bo Yang, was born in Linwu, Ningxia, P.R. China in 1972. He received B.S and M.S degrees in Electrical Engineering from Tsinghua University, Beijing, China respectively.

In fall 1997, the author joined the Virginia Power Electronics Center (VPEC) - now the Center for Power Electronics Systems (CPES) - at Virginia Polytechnic Institute and State University, Blacksburg, Virginia. His research interests include power converter simulation and modeling, magnetic design and modeling, DC/DC converters, and voltage regulator modules (VRMs).

The author is a member of the IEEE Power Electronics Society.